On the Structural Basis for Size-selective Permeation of Organic Cations through the Voltage-gated Sodium Channel

Effect of Alanine Mutations at the DEKA Locus on Selectivity, Inhibition by Ca^{2+} and H^+, and Molecular Sieving

YE-MING SUN,* ISABELLE FAVRE,* LAURENT SCHILD,‡ and EDWARD MOCZYDLOWSKI*§

From the *Department of Pharmacology, and §Department of Cellular and Molecular Physiology, Yale University Medical School, New Haven, Connecticut 06520-8066; and ‡Institut de Pharmacologie et Toxicologie, de l'Universite de Lausanne, CH-1005 Lausanne, Switzerland

ABSTRACT Recent evidence indicates that ionic selectivity in voltage-gated Na^+ channels is mediated by a small number of residues in P-region segments that link transmembrane elements S5 and S6 in each of four homologous domains denoted I, II, III, and IV. Important determinants for this function appear to be a set of conserved charged residues in the first three homologous domains, Asp(I), Glu(II), and Lys(III), located in a region of the pore called the DEKA locus. In this study, we examined several Ala-substitution mutations of these residues for alterations in ionic selectivity, inhibition of macroscopic current by external Ca^{2+} and H^+, and molecular sieving behavior using a series of organic cations ranging in size from ammonium to tetraethylammonium. Whole-cell recording of wild-type and mutant channels of the rat muscle μ1 Na^+ channel stably expressed in HEK293 cells was used to compare macroscopic current–voltage behavior in the presence of various external cations and an intracellular reference solution containing Cs^+ and very low Ca^{2+}. In particular, we tested the hypothesis that the Lys residue in domain III of the DEKA locus is responsible for restricting the permeation of large organic cations. Mutation of Lys(III) to Ala largely eliminated selectivity among the group IA monovalent alkali cations (Li^+, Na^+, K^+, Rb^+, Cs^+) and permitted inward current of group IIA divalent cations (Mg^{2+}, Ca^{2+}, Sr^{2+}, Ba^{2+}). This same mutation also resulted in the acquisition of permeability to many large organic cations such as methylammonium, tetramethylammonium, and tetraethylammonium, all of which are impermeant in the native channel. The results lead to the conclusion that charged residues of the DEKA locus play an important role in molecular sieving behavior of the Na^+ channel pore, a function that has been previously attributed to a hypothetical region of the channel called the "selectivity filter." A detailed examination of individual contributions of the Asp(I), Glu(II), and Lys(III) residues and the dependence on molecular size suggests that relative permeability of organic cations is a complex function of the size, charge, and polarity of these residues and cation substrates. As judged by effects on macroscopic conductance, charged residues of the DEKA locus also appear to play a role in the mechanisms of block by external Ca^{2+} and H^+, but are not essential for the positive shift in activation voltage that is produced by these ions.

KEY WORDS: Ca^{2+} channel • ionic selectivity • μ-conotoxin • Na^+ channel • selectivity filter

INTRODUCTION

Channel proteins are generally known for mediating transmembrane currents of the major inorganic ions of physiological solutions. However, many channels also allow permeation of small organic ions and polar nonelectrolytes. In this respect, channel pores exhibit sieving behavior much like a dialysis membrane or gel filtration material designed to exhibit a well-defined molecular weight cutoff. As reviewed by Hille (1992), this latter property has been widely used to estimate the minimum diameter of channel pores as deduced from the size of the largest ions that serve as current carriers in electrophysiological assays. For example, cross-sectional areas corresponding to the molecular cutoff region of various members of the superfamily of voltage-gated ion channels have been estimated as follows: voltage-gated K^+ channel, 3.3 × 3.3 Å (Bezanilla and Armstrong, 1972; Hille, 1973); voltage-gated Na^+ channel, 3.2 × 5.2 Å (Hille, 1971, 1972); and voltage-gated Ca^{2+} channel, 5.5 × 5.5 Å (McCleskey and Almers, 1985; Coronado and Smith, 1987).

Despite a lack of high resolution structures of channel proteins, there is now much information regarding

Address correspondence to Edward Moczydlowski, Department of Pharmacology, Yale University School of Medicine, 333 Cedar St., New Haven, CT 06520-8066. Fax: 203-785-7670; E-mail: edward.moczydlowski@yale.edu

which amino acid residues are likely to form the pore region for several types of channels. This has motivated attempts to determine the relationship between amino acid side chains thought to form the lining or selectivity region of channel pores, and the molecular cutoff behavior with respect to organic ions (Cohen et al., 1992; Wang and Imoto, 1992; Goulding et al., 1993). In this paper, we address a specific question along these lines for the voltage-gated Na^+ channel of rat skeletal muscle: do key residues that are known to determine ionic selectivity among Na^+, K^+, and Ca^{2+} also control the size-selective permeation of organic cations?

Voltage-gated Na^+ and Ca^{2+} channels are homologous proteins that differ in their ionic selectivity. Native Na^+ channels are at least 10-fold more permeable to Na^+ than K^+ and are virtually impermeable to Ca^{2+} (Hille, 1972; Campbell, 1976; Pappone, 1980). Ca^{2+} channels are highly selective for group IIA divalent cations (Ca^{2+}, Sr^{2+}, Ba^{2+}), but also exhibit nonselective currents of Na^+ or K^+ when the concentration of Ca^{2+} is quite low (<1 μM) (Kuo and Hess, 1993; Almers and McCleskey, 1984; Almers et al., 1984; Hess and Tsien, 1984). Site-directed mutagenesis experiments have revealed that the structural basis for this ion discrimination is primarily specified by a conserved motif of four amino acid residues, one in each of the four internally homologous domains that comprise the α subunit of pseudo-tetrameric Na^+ and Ca^{2+} channels (Heinemann et al., 1992; Kim et al., 1993; Tang et al., 1993; Yang et al., 1993; Ellinor et al., 1995; Parent and Gopalakrishnan, 1995). This motif consists of the following residues in domains I–IV: Asp(I), Glu(II), Lys(III), Ala(IV) in Na^+ channels, and Glu(I), Glu(II), Glu(III), Glu(IV) in Ca^{2+} channels, respectively denoted as the DEKA and EEEE locus. From previous studies of Na^+ channels expressed in *Xenopus* oocytes, it may be inferred that the Lys(III) residue of the Na^+ channel DEKA motif is an especially important determinant of the characteristic ionic selectivity of this channel. Na^+ channel mutagenesis experiments conducted thus far suggest that Lys(III) is primarily responsible for excluding the permeation of divalent cations such as Ca^{2+} and is also specifically required for Na^+/K^+ discrimination (Heinemann et al., 1992; Favre et al., 1996; Schlief et al., 1996; Chen et al., 1997; Tsushima et al., 1997).

Since the side chain of the Na^+ channel Lys(III) residue has an opposite charge and is significantly larger than the corresponding Glu(III) residue of the Ca^{2+} channel, we previously speculated that this residue might also play an important role in molecular cut-off behavior (Favre et al., 1996). From classic studies, the largest organic cations observed to carry inward current in native Na^+ channels are guanidine, aminoguanidine, and hydroxyguanidine (Hille, 1971; Campbell, 1976; Pappone, 1980). In contrast, larger cations such as tetramethylammonium (TMA)[1] and possibly even tetraethylammonium (TEA) have been found to permeate through Ca^{2+} channels in the absence of Ca^{2+} (McCleskey and Almers, 1985; Coronado and Smith, 1987). Therefore, the hypothesis that Lys(III) accounts for the smaller cutoff diameter of Na^+ channels versus Ca^{2+} channels predicts that mutation of Lys(III) to a small neutral residue such as Ala should increase the permeability of organic cations.

To test this hypothesis and further examine the proposal that the DEKA locus functions as a "selectivity filter" (Heinemann et al., 1992, 1994; Schlief et al., 1996), we measured the relative permeability of various inorganic and organic cations for the wild-type μ1 Na^+ channel and several Ala mutations of the DEKA locus stably expressed in cultured HEK293 cells. Since mutations of charged residues in the pore could potentially affect the sensitivity of the channel to inhibition by external Ca^{2+} and H^+ (Chen et al., 1996; Schlief et al., 1996), we also compared the macroscopic Ca^{2+} dependence and pH dependence of the wild-type, DEAA, and AAAA channels. Whole-cell voltage-clamp recording was used to analyze macroscopic current–voltage behavior for different extracellular solutions and an intracellular reference solution containing Cs^+ as the major cation. As observed in similar work using *Xenopus* oocytes (Heinemann et al., 1992; Favre et al., 1996; Schlief et al., 1996; Chen et al., 1997; Tsushima et al., 1997), we found that mutation of the Lys(III) residue to Ala (DEAA mutant) practically eliminates ionic selectivity among group IA alkali cations (Li^+, Na^+, K^+, Rb^+, and Cs^+) and confers permeability to group IIA divalent cations (Mg^{2+}, Ca^{2+}, Sr^{2+}, Ba^{2+}). We found that the sensitivity of the AAAA mutant to inhibition of macroscopic conductance by Ca^{2+} and H^+ was diminished in comparison with the wild-type channel, implying that at least part of the normal blocking action of external Ca^{2+} and H^+ occurs at the DEKA locus. The Lys(III) to Ala substitution also confers permeability to many large organic cations such as methylammonium, TMA, and TEA, which cannot conduct current through the native channel. Ala substitution of the acidic residues, Asp(I) and Glu(II), showed that in the Lys(III) to Ala(III) background, these negatively charged residues of the DEKA locus cooperate to facilitate the permeation of divalent cations and large organic cations. Our findings clearly identify the DEKA locus as a region of the channel that functions in molecular filtration as well as selectivity for inorganic ions. However, by com-

[1]*Abbreviations used in this paper:* DMA, dimethylamine; EA, ethylamine; EAOH, ethanolamine; MA, methylamine; STX, saxitoxin; TEA, tetraethylammonium; TMA, tetramethylammonium; TriMA, trimethylamine; TTX, tetrodotoxin.

paring the sieving properties of different mutants, it appears that size-selective molecular filtration is not simply a mechanical property governed by the side chain volume of residues at the DEKA locus and the size of cation substrates. As concluded in earlier work (Hille, 1972), other factors such as chemical and electrostatic interactions may also play a role in determining the relative permeability of organic cations.

MATERIALS AND METHODS

Mutations, Subcloning, and Stable Transfection in the HEK293 Cell Line

The Na^+ channel variants studied here are derived from cDNA encoding the μ1 rat skeletal muscle isoform (Trimmer et al., 1989) cloned into the EcoRI site of pBluescript SK^+ as originally obtained from Dr. W.S. Agnew (Department of Physiology, Johns Hopkins University School of Medicine, Baltimore, MD). In this work, we used native μ1 and four Ala-substitution mutations of the DEKA locus called DEAA, DAAA, AEAA, and AAAA, which have been previously characterized in the *Xenopus* oocyte expression system (Favre et al., 1996). The site-directed mutations, D400A, E755A, and K1237A, in homologous domains I, II, and III, respectively, were introduced into the μ1 clone in the pBluescript vector using PCR methodology and verified by sequencing as described in Favre et al. (1995). Full-length Na^+ channel cDNA for wild type and mutants was subcloned into the mammalian cell expression vector pcDNA3 at the EcoRI site (Invitrogen Corp., San Diego, CA).

HEK293 cells were transfected with the μ1/pcDNA3 vector for wild type and mutants using the calcium phosphate precipitation method (Chen and Okayama, 1987). HEK293 cells were maintained at 37°C in Dulbecco's Modified Eagle's Medium supplemented with 10% fetal bovine serum, 100 U/ml penicillin G, and 100 μg/ml streptomycin. Transfected cells were selected for neomycin resistance in 700 μg/ml G418. Approximately 10 d after transfection, single-cell colonies were picked and assayed by whole cell patch clamp to locate those colonies with high-level expression. Such colonies were propagated and maintained as stably transfected cell lines in the presence of 500 μg/ml G418. Cells were seeded for growth on cover slips and used for electrophysiological recording after 2–3 d. HEK293 cells expressing the wild-type μ1 channel typically exhibited a maximum peak Na^+ current of ~5 nA. The other mutants exhibited a lower level of peak Na^+ current in the range of ~1–3 nA.

Electrophysiology

Patch clamp electrodes were fabricated on a PP-83 two-stage electrode puller (Narishige USA, Inc., Glen Cove, NY) using Kimax 50 borosilicate glass (Fisher Scientific Co., Pittsburgh, PA). After fire polishing, the pipette resistance was 2–4 MΩ when filled with standard pipette solution. Whole-cell voltage clamp recording was performed at room temperature (~22°C) using a HEKA EPC-9 amplifier with Pulse and Pulse-fit acquisition and analysis software (Instrutech, Great Neck, NY). To minimize space-clamp problems, only isolated cells with an average diameter in the range of 10–30 μm were selected for recording. Cells were not accepted for recording if the initial seal resistance was <5 GΩ or if the peak Na^+ current was <1 nA. Voltage errors were minimized using series resistance compensation (generally 80%). Cancellation of the capacitance transients and leak subtraction was performed using a programmed P/4 protocol delivered at −120 mV. The quality of the clamp was judged according to the criteria of Armstrong and Gilly (1992). Membrane currents were filtered at 5 kHz.

Current–voltage data were typically collected by recording responses to a consecutive series of step pulses from a holding potential of −120 mV at intervals of +5 mV beginning at −90 mV (pulse duration = 10 ms, pulse frequency = 1 Hz). Data collection was initiated ~5 min after break-in when control Na^+ currents had stabilized after intracellular perfusion with pipette solution. Data was always recorded during continuous perfusion of the clamped cell with extracellular solution. Permeability to different cations was tested by recording an I–V sequence, first in control Na^+ solution, and then during perfusion with a solution of the test cation, and again after replacement with control Na^+ solution. Cation effects reported in this study were reversible as determined by complete recovery of the control Na^+ currents. The pipette electrode was zeroed in control Na^+ solution before patching a cell. After completing a recording, the cell was dislodged by applying positive pressure to the pipette. The change in potential was then measured for each test solution relative to the Na^+ control solution. These values, normally <5 mV, were subtracted from the applied voltages for the various test solutions to correct for changes in junction potential.

Solutions and Materials

For all experiments with Cs^+-permeable Na^+ channel mutants (DEAA, DAAA, AEAA, AAAA), the following intracellular (pipette) solution was used (mM): 130 CsF, 1 $MgCl_2$, 5 EGTA, 10 HEPES, adjusted to pH 7.3 with CsOH. For all experiments with the Cs^+-impermeable wild-type Na^+ channel, this pipette solution was modified as follows to include 20 mM Na^+, which permits recording of outward current and an accurate measurement of the reversal potential (mM): 120 CsF, 1 $MgCl_2$, 5 EGTA, 20 Na-HEPES, adjusted to pH 7.3 with CsOH. The standard control extracellular (bath) solution was: 140 NaCl, 2.5 KCl, 2 $MgCl_2$, 1 $CaCl_2$, 10 glucose, 10 HEPES, adjusted to pH 7.3 with NaOH. For experiments testing permeability to Li^+, K^+, Rb^+, Cs^+, and various monovalent organic cations, 140 mM NaCl in the standard extracellular solution was replaced by 140 mM Cl^--salt of the test cation and the NaOH used to titrate the buffer was replaced either by the hydroxide salt of the test cation or Tris base. For experiments testing permeability to Ca^{2+}, Mg^{2+}, Sr^{2+}, and Ba^{2+}, standard extracellular 140 mM NaCl was replaced by 90 mM Cl^-_2 salt of the test cation and NaOH was replaced by Tris base. For the experiments of Fig. 3, testing the effect of external Ca^{2+} on Na^+ current, Ca^{2+} was varied by using standard solution with 100 mM NaCl and the following mixtures of $CaCl_2$/Tris-Cl, at pH 7.3 (mM): 1/40, 3.5/37.5, 6/35, 11/30, 21/20, 31/10. For the experiments of Fig. 4, testing the effect of extracellular pH, standard 140 mM NaCl solution was used and pH was varied in the range of 4.0–8.0 by adjustment with HCl or Tris base as required. All solutions were filtered with a 0.22-μm filter before use. The external recording solution in the experimental chamber was continuously exchanged by a gravity-driven flow/suction arrangement at rate of ~1 ml/min. With a chamber volume of ~1 ml, 3–5 min was allowed for complete exchange of external solution before data collection.

Chemicals used for permeability measurements were from the following sources: NaCl, KCl, and NH_4Cl (J.T. Baker, Inc., Phillipsburg, NJ); LiCl, CH_3NH_2·HCl, $(CH_3)_2NH$·HCl, $(CH_3)_3N$·HCl, $(CH_3)_4N^+OH^-$, $CH_3CH_2NH_2$ (liquid), $CH_2OHCH_2NH_2$ (liquid), cholineCl, $(CH_3CH_2)_4N^+Cl^-$, guanidineHCl, aminoguanidine·1/2(H_2SO_4), and methylguanidine·1/2(H_2SO_4) (Sigma Chemical Co., St. Louis, MO); RbCl, CsF, CsCl, $MgCl_2·6H_2O$, $SrCl_2·6H_2O$, and $BaCl_2·6H_2O$ (Alfa, Ward Hill, MA); $CaCl_2·2H_2O$ (Fisher, Pittsburgh, PA), NH_2OH·HCl (Eastman Kodak Co., Rochester,

NY), and Tris (American Bioanalytical, Natick, MA). Tetrodotoxin and saxitoxin were purchased from Calbiochem Corp. (San Diego, CA). μ-Conotoxin GIIIB was obtained from Bachem (King of Prussia, PA).

Data Analysis

Macroscopic I–V parameters were obtained by fitting peak current–voltage data to the following transform of a Boltzmann function:

$$I = \frac{G_{max}(V - V_R)}{1 + \exp\{(V - V_{0.5})/k\}}, \quad (1)$$

where I is the peak current, V is the test voltage, V_R is the reversal potential, G_{max} is the maximal conductance, $V_{0.5}$ is the midpoint voltage for activation, and k is a slope factor. In cases where no inward current was observed, an upper limit for the reversal potential was estimated by extrapolation of the smallest values of outward current to the voltage axis.

The DEAA and AAAA mutants were tested for permeability to anions by replacing Cl^- in the external solution with acetate or sulfate in the presence of a weakly permeant cation such as Tris. The results indicated that Cl^-/F^- permeability is negligible relative to cations. Thus, anions were ignored in permeability calculations. The permeability ratio of any monovalent test cation, X^+, was computed relative to Na^+ from the change in the reversal potential observed in going from control external Na^+ solution (subscript 1) to external X^+ solution (subscript 2) according to (Hille, 1971):

$$\frac{P_X}{P_{Na}} = \frac{[Na]_1}{[X]_2}\exp\left(\frac{\Delta V}{\alpha}\right), \quad (2)$$

where $\Delta V = V_2 - V_1$, and $\alpha = RT/F = 25.4$ mV. The permeability ratio of Ca^{2+} and other divalent cations was similarly estimated as previously described (Favre et al., 1996) from changes in reversal potential in going from control Na^+ solution (subscript 1) to Ca^{2+} solution (subscript 2) according to the following equation, derived from the extended Goldman-Hodgkin-Katz equation (Lewis, 1979):

$$\frac{P_{Ca}}{P_{Na}} = \frac{\left\{\exp\left(\frac{\Delta V}{\alpha}\right)\right\}\left\{[Na]_1 + \frac{P_K}{P_{Na}}[K]_1\right\} - \frac{P_K}{P_{Na}}[K]_2}{4\left\{\frac{[Ca]_2}{1 + \exp(V_2/\alpha)} - \frac{[Ca]_1\exp(\Delta V/\alpha)}{1 + \exp(V_1/\alpha)}\right\}}. \quad (3)$$

Activity coefficients required for calculating the activity of the various ionic species in Eqs. 2 and 3 were based on the Davies equation as described previously (Favre et al., 1996). In calculating the permeability ratio of hydroxylammonium at pH 6, a pKa of 5.95 (Hille, 1971) was used to determine the cation concentration. Other amines were assumed to be fully protonated at pH 7.3.

Nonlinear regression fitting of data to Eq. 1 and other equations given in the text was performed using the Marquardt-Levenberg algorithm of Sigmaplot 3.0 software (SPSS Inc., Chicago IL). Molecular models of organic cations were constructed and energy minimized with the use of Hyperchem software (Hypercube Inc., Waterloo, Ontario, Canada). The smallest diameter of a circular hole through which various organic cations can pass (listed in Table II) was estimated using the Select Sphere function of Hyperchem. The van der Waals volume of organic cations and various amino acid side chains was measured using Insight software (Biosym, San Diego, CA).

RESULTS

In previous work on mutational analysis of μ1 Na^+ channel selectivity (Favre et al., 1996), we used the *Xenopus* oocyte expression system. For the present studies on organic cation permeation, we switched to a mammalian cell line (HEK293) expression system to control the composition of the intracellular solution with a well-buffered low Ca^{2+} solution in order to avoid various complications in interpretation arising from activation of endogenous currents present in *Xenopus* oocytes (Schlief et al., 1996), and to allow for higher fidelity whole cell recording. Before presenting results on organic cation permeation, this paper first documents the behavior of selected mutants expressed in HEK293 cells with respect to monovalent and divalent inorganic cations. These experiments recapitulate basic findings already reported for Na^+, K^+, and Ca^{2+} in oocytes (Favre et al., 1996) and also provide new selectivity information on the congener ions, Li^+, Rb^+, Cs^+, Mg^{2+}, Sr^{2+}, and Ba^{2+}. From previous work on Ca^{2+} (Ellinor et al., 1995; Chen et al., 1996) and Na^+ (Heinemann et al., 1992) channels, it is clear that mutations at the DEKA locus may affect blocking interactions mediated by omnipresent extracellular Ca^{2+} and H^+. Thus, as control experiments to assess whether these effects would be important for subsequent interpretations, results on Ca^{2+} and H^+ inhibition are also presented before the molecular sieving studies.

Selectivity for Group IA Alkali Cations

As described in MATERIALS AND METHODS, HEK293 cell lines were established that stably express the wild-type μ1 Na^+ channel and the following single, double, and triple Ala-substitution mutations of the DEKA locus: DEAA, DAAA, AEAA, and AAAA. We previously found that voltage-activated currents nonselective for Na^+ and K^+ are observed when these particular channel mutations are expressed in *Xenopus* oocytes (Favre et al., 1996). Fig. 1 illustrates the selectivity behavior of these mutants expressed in HEK293 cells with respect to the monovalent alkali cations, Li^+, Na^+, K^+, Rb^+ and Cs^+. Macroscopic currents elicited by a series of step depolarizations from a holding voltage of −120 mV were recorded in a control extracellular solution containing 140 mM NaCl before and after perfusion with a test solution in which extracellular Na^+ was substituted by a different alkali cation. The intracellular (pipette) solution contained either 130 mM Cs^+ as the major cation for the various mutants or 120 mM Cs^+ plus 20 mM Na^+ for the wild-type DEKA channel. Typical voltage-activated currents shown in Fig. 1 *A* are normalized to the maximal peak Na^+ current from the same cell.

The results of Fig. 1 *A* show that a very small inward current is observed for the wild-type (DEKA) channel when extracellular Na^+ is replaced by K^+, and virtually no inward current is observed in the presence of extracellular Cs^+. This is expected from the high Na^+ selectivity of the native channel. Na^+ (20 mM) in the pipette

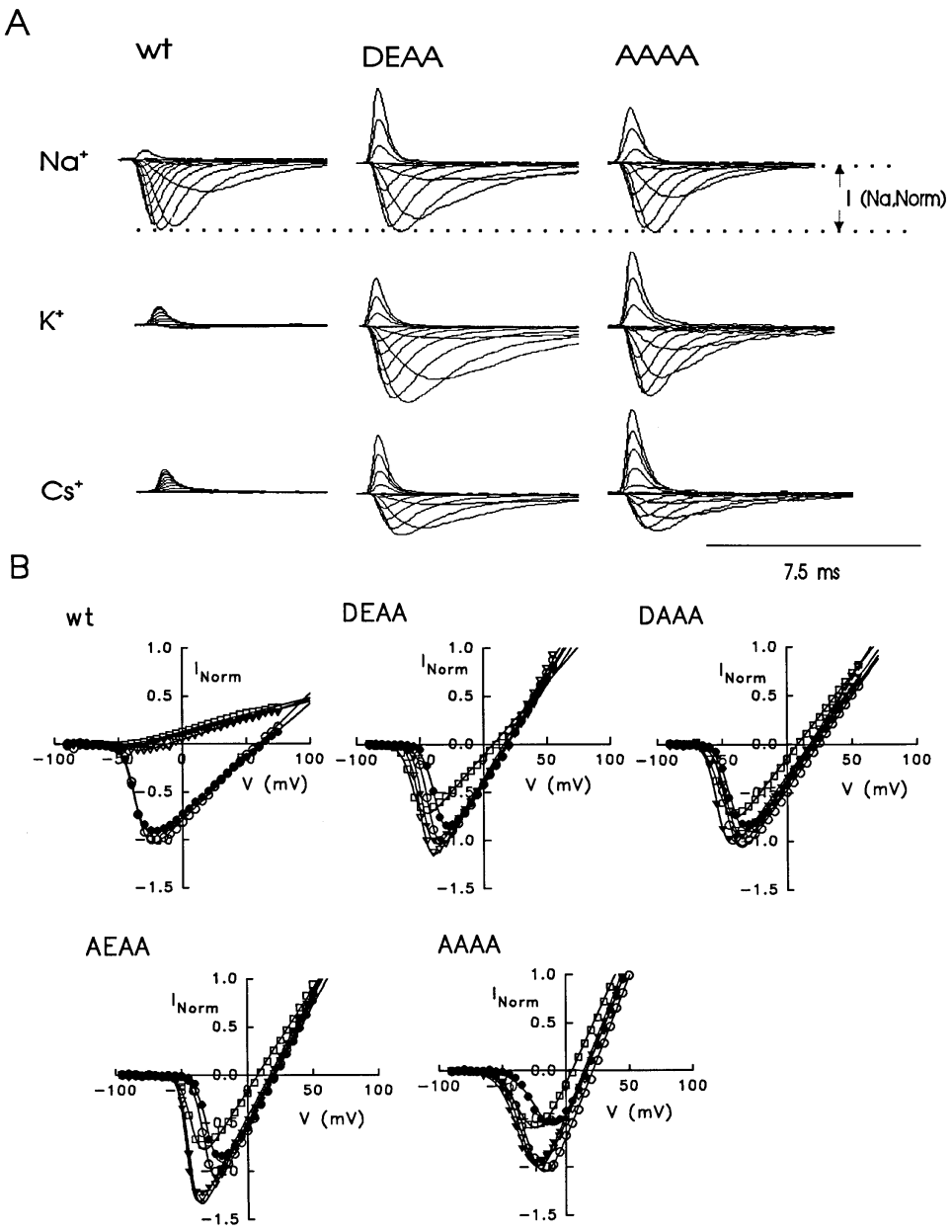

FIGURE 1. Comparison of group IA monovalent cation permeation in μ1 wild-type (*wt*) and mutant Na^+ channels expressed in HEK293 cells. (*A*) Typical currents recorded in the presence of extracellular Na^+, K^+, or Cs^+ for wild-type, DEAA, and AAAA mutants. Currents shown were elicited from a holding voltage of −120 mV by step depolarizations ranging from –90 to +50 mV in steps of 10 mV. Currents from each cell are normalized to the peak Na^+ current from the same cell recorded in control Na^+ solution as indicated by the vertical scale labeled I (Na,Norm). (*B*) Normalized peak I–V relations for typical cells expressing wild-type, DEAA, DAAA, AEAA, or AAAA mutants. Solid line curves indicate fits to a Boltzmann function (Eq. 1). Data for the following group IA monovalent cation solutions (140 mM Cl^- salts) are superimposed: Na^+ (○), Li^+ (●), K^+ (▽), Rb^+ (▼), and Cs^+ (□).

solution allows small outward currents to be recorded for the wild-type channel under these conditions. In contrast to this behavior, the DEAA and AAAA mutants exhibit large inward and outward currents when extracellular Na^+ is substituted by K^+ or Cs^+. This reflects a profound alteration of ionic selectivity as previously observed in the oocyte expression system (Favre et al., 1996).

Fig. 1 *B* shows a comparison of typical peak I–V data normalized to the peak Na^+ current for the wild-type and four mutants. For extracellular Na^+ and Li^+, the DEKA channel exhibits similar inward currents and I–V behavior, as expected from the characteristic behavior of native Na^+ channels (Hille, 1972). The larger ions, K^+, Rb^+, and Cs^+, are much less permeant through the wild-type channel as indicated by low or absent inward current. In contrast, each of the four mutant channels exhibits a similar reversal potential for Na^+, Li^+, K^+, and Rb^+. These results are summarized in Table I, which lists the permeability ratio (P_X/P_{Na}) calculated from the change in reversal potential together with the relative maximal inward current (I_X/I_{Na}). For all four mutants, there is very little discrimination among Na^+, Li^+, K^+, and Rb^+ since P_X/P_{Na} is close to 1.0 for all of these ions. The large Cs^+ ion is about half as permeable as the other cations for the mutants with P_{Cs}/P_{Na} in the range of 0.49–0.57. In general, lack of ion discrimination by the various mutants is similarly reflected by the relative magnitudes of peak inward currents (I/I_{Na}) for the various alkali cations (Table I). The experiments of

TABLE I

Selectivity Properties of Wild-Type and Mutant Na^+ Channels for Inorganic Cations

Parameter		DEKA (wt)	DEAA	DAAA	AEAA	AAAA
Na^+	V_R	56.2 ± 2.1 (23)	23.0 ± 4.8 (28)	23.0 ± 1.7 (11)	20.7 ± 0.8 (12)	24.4 ± 1.5 (32)
	P/P_{Na}	1	1	1	1	1
	I/I_{Na}	1	1	1	1	1
Li^+	V_R	58.9 ± 2.9 (3)	23.5 ± 2.8 (5)	20.7 ± 0.5 (3)	23.1 ± 4.0 (4)	14.7 ± 3.2 (4)
	P/P_{Na}	1.03 ± 0.11	1.17 ± 0.11	0.92 ± 0.04	0.99 ± 0.06	0.74 ± 0.07
	I/I_{Na}	0.83 ± 0.01	0.84 ± 0.01	0.81 ± 0.02	0.82 ± 0.01	0.55 ± 0.01
K^+	V_R	−3.6 ± 2.8 (3)	16.2 ± 2.7 (4)	17.2 ± 1.9 (3)	21.9 ± 3.5 (3)	20.7 ± 2.1 (4)
	P/P_{Na}	0.08 ± 0.01	0.87 ± 0.04	0.81 ± 0.05	0.91 ± 0.03	0.94 ± 0.04
	I/I_{Na}	0.07 ± 0.01	1.11 ± 0.04	0.91 ± 0.14	1.25 ± 0.10	1.00 ± 0.03
Rb^+	V_R	<−30.3 ± 1.4 (3)	17.0 ± 1.7 (3)	17.4 ± 0.3 (3)	19.5 ± 3.3 (3)	18.0 ± 2.6 (3)
	P/P_{Na}	<0.03	0.83 ± 0.13	0.80 ± 0.06	0.83 ± 0.04	0.83 ± 0.02
	I/I_{Na}	<0.01	0.97 ± 0.10	1.07 ± 0.11	1.22 ± 0.10	0.94 ± 0.02
Cs^+	V_R	<−53.7 ± 2.6 (3)	6.3 ± 1.6 (3)	8.5 ± 0.4 (3)	9.9 ± 3.4 (4)	4.6 ± 1.2 (4)
	P/P_{Na}	<0.01	0.57 ± 0.02	0.57 ± 0.03	0.56 ± 0.03	0.49 ± 0.05
	I/I_{Na}	<0.01	0.65 ± 0.03	0.71 ± 0.04	0.73 ± 0.05	0.62 ± 0.02
Ca^{2+}	V_R	<−13.1 ± 0.3 (4)	45.7 ± 3.2 (5)	25.7 ± 6.8 (2)	37.0 ± 1.6 (3)	<−14.3 ± 2.8 (3)
	P/P_{Na}	<0.09	25.2 ± 8.6	4.33 ± 1.17	12.5 ± 1.4	<0.38
	I/I_{Na}	<0.01	0.57 ± 0.02	0.13 ± 0.01	0.24 ± 0.01	<0.01
Mg^{2+}	V_R	<−13.1 ± 0.3 (3)	37.0 ± 4.5 (5)	3.1 ± 0.9 (2)	22.6 ± 1.3 (3)	<−24.4 ± 1.4 (3)
	P/P_{Na}	<0.1	12.8 ± 3.9	0.98 ± 0.25	4.44 ± 0.29	<0.22
	I/I_{Na}	<0.01	0.22 ± 0.03	0.03 ± 0.01	0.08 ± 0.01	<0.01
Sr^{2+}	V_R	<−13.0 ± 0.4 (4)	36.9 ± 6.8 (3)	3.3 ± 0.8 (2)	20.6 ± 3.0 (2)	<−34.4 ± 2.9 (5)
	P/P_{Na}	<0.1	11.9 ± 5.4	0.96 ± 0.12	3.98 ± 0.76	<0.13
	I/I_{Na}	<0.01	0.16 ± 0.01	0.05 ± 0.01	0.06 ± 0.01	<0.01
Ba^{2+}	V_R	<−13.0 ± 0.3 (4)	22.6 ± 0.1 (2)	−3.1 ± 0.2 (2)	19.0 ± 2.0 (2)	<−38.3 ± 3.3(4)
	P/P_{Na}	<0.09	4.31 ± 0.31	0.65 ± 0.12	3.56 ± 0.43	<0.10
	I/I_{Na}	<0.01	0.02 ± 0.02	0.01 ± 0.01	0.01 ± 0.01	<0.01

All values are means ± SD with the number of experiments in parenthesis. V_R is the mean reversal potential in millivolts measured for each cation. In cases where inward current was not detected, estimated upper limits for V_R and P/P_{Na} are given. Permeability ratios (P/P_{Na}) for each cation were calculated according to Eqs. 2 or 3 from paired changes in V_R measured for a given cell perfused first with control Na^+ solution and after replacement with the test cation solution. I/I_{Na} was measured as the ratio of maximum peak inward current observed for the test cation to that for observed Na^+ in the same cell.

Fig. 1 thus confirm that these four mutants of the DEKA locus are defective in their ability to differentiate among all monovalent alkali cations, a physiologically essential function of the native Na^+ channel. The data also confirm that the single substitution of the Lys residue in domain III by Ala is sufficient to cause this drastic alteration. The additional Ala substitutions in domains I and II have little effect on the weak alkali cation selectivity observed in the DEAA background.

Selectivity for Group IIA Divalent Cations

Using the oocyte expression system, we previously found that substitution of the Lys residue in the domain III position of the DEKA locus by various neutral residues (Ala, Cys, Met, Phe, and His, at pH 7.2) greatly enhanced Ca^{2+} permeation (Favre et al., 1996). However, the quantitative measurement of Ca^{2+} current was complicated by the presence of endogenous Ca^{2+}-activated Cl^- currents in *Xenopus* oocytes (Heinemann et al., 1992). A cleaner characterization of this phenomenon can be performed in the HEK293 cell expression system, since these fibroblastlike cells do not exhibit significant endogenous currents that are activated or carried by Ca^{2+}. Fig. 2 *A* shows typical current records obtained in the presence of 90 mM extracellular $CaCl_2$ or $MgCl_2$ for wild type, DEAA, and AAAA. Voltage-activated inward currents observed for the DEAA mutant demonstrate that this channel is permeable to both Ca^{2+} and Mg^{2+}. The absence of inward currents and the rapidly inactivating outward currents carried by internal Na^+ for the wild-type channel (20 mM Na^+ in the pipette solution) or by internal Cs^+ for the AAAA mutant confirm that these two channels are quite impermeable to extracellular divalent cations (Favre et al., 1996).

Fig. 2 *B* shows a detailed comparison of peak I–V behavior in the presence of external Ca^{2+}, Mg^{2+}, Sr^{2+}, or Ba^{2+}. Of the four divalent cations, Ca^{2+} carries the largest current through the DAAA, AEAA, and DEAA chan-

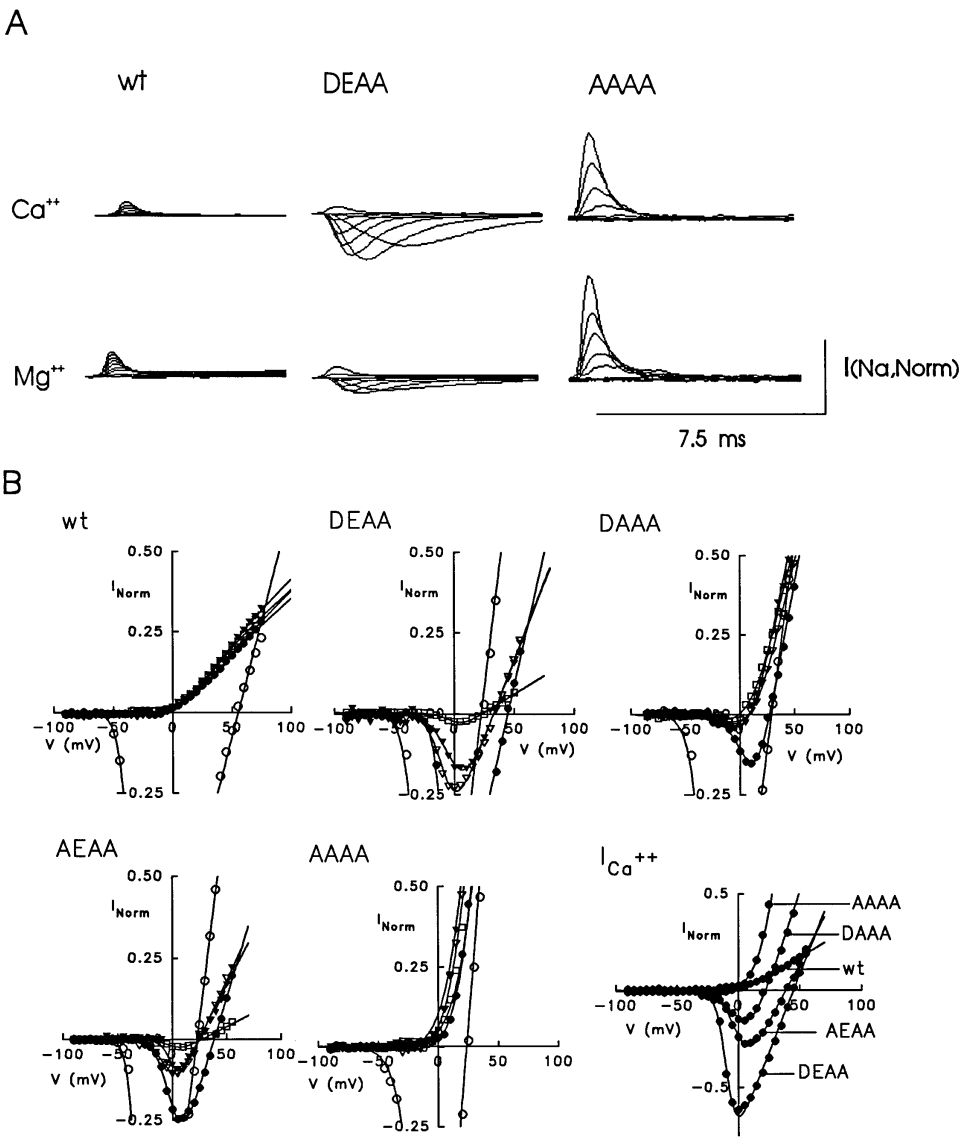

FIGURE 2. Comparison of group IIA divalent cation permeation in wild-type and mutant Na^+ channels. (*A*) Typical currents recorded in the presence of extracellular Ca^{2+} or Mg^{2+} for wild-type, DEAA, and AAAA mutants. Currents were activated by the same voltage protocol described in Fig. 1. The vertical calibration is 1× for normalized peak Na^+ current. (*B*) Normalized peak I–V relations and Boltzmann fits (*solid lines*) for typical cells expressing wild-type, DEAA, DAAA, AEAA, or AAAA mutants. Data recorded in Na^+ and the following group IIA divalent cation solutions (90 mM) are superimposed: Na^+ (○), Ca^{2+} (●), Mg^{2+} (▽), Sr^{2+} (▼), and Ba^{2+} (□). The current scale is truncated to magnify results for divalent cations. The lower right panel shows normalized peak I–V data for Ca^{2+} as compared with the wild-type and indicated mutants.

nels. In particular, the DEAA channel exhibits the largest relative inward Ca^{2+} current, followed by AEAA and DAAA (see comparison of I_{Ca} in Fig. 2 *B, bottom right*). Measured reversal potentials in the presence of Na^+ and Ca^{2+} can be used to calculate P_{Ca}/P_{Na} (using Eq. 3) as follows: DEAA, 25.2; AEAA, 12.5; DAAA, 4.3; AAAA < 0.38. These values are similar to those obtained for somewhat different ionic conditions using *Xenopus* oocytes (Favre et al., 1996). Under the present conditions, Ba^{2+} is generally the least permeant group IIA cation for the three Ca^{2+}-permeable mutants. The relative permeability of Mg^{2+} and Sr^{2+} is similar in these mutants as judged by the measured maximal inward current and the calculated permeability ratios (Table I). The experiments of Fig. 2 support the previous conclusion (Favre et al., 1996) that substitution of the Lys(III) residue by Ala renders the channel permeable to group IIA divalent cations and that this functional ability is also dependent on the presence of at least one of the acidic residues, Asp(I) and Glu(II), of the DEKA locus.

Blocking and Gating-shift Effect of External Ca^{2+}

Previous work has shown that mutations of the DEKA locus in the rat brain II Na channel may influence the blocking affinity as well as the permeability of extracellular divalent cations (Heinemann et al., 1992). In particular, the apparent blocking affinity for inhibition of Na^+ current by extracellular Ca^{2+} is closely correlated with the net negative charge of residues at the four DEKA positions (Schlief et al., 1996). These latter researchers have also found that the peak inward Na^+ current for the DEEA and EEEE mutants is strongly inhibited by extracellular Ca^{2+} in the range of 1–100 μM,

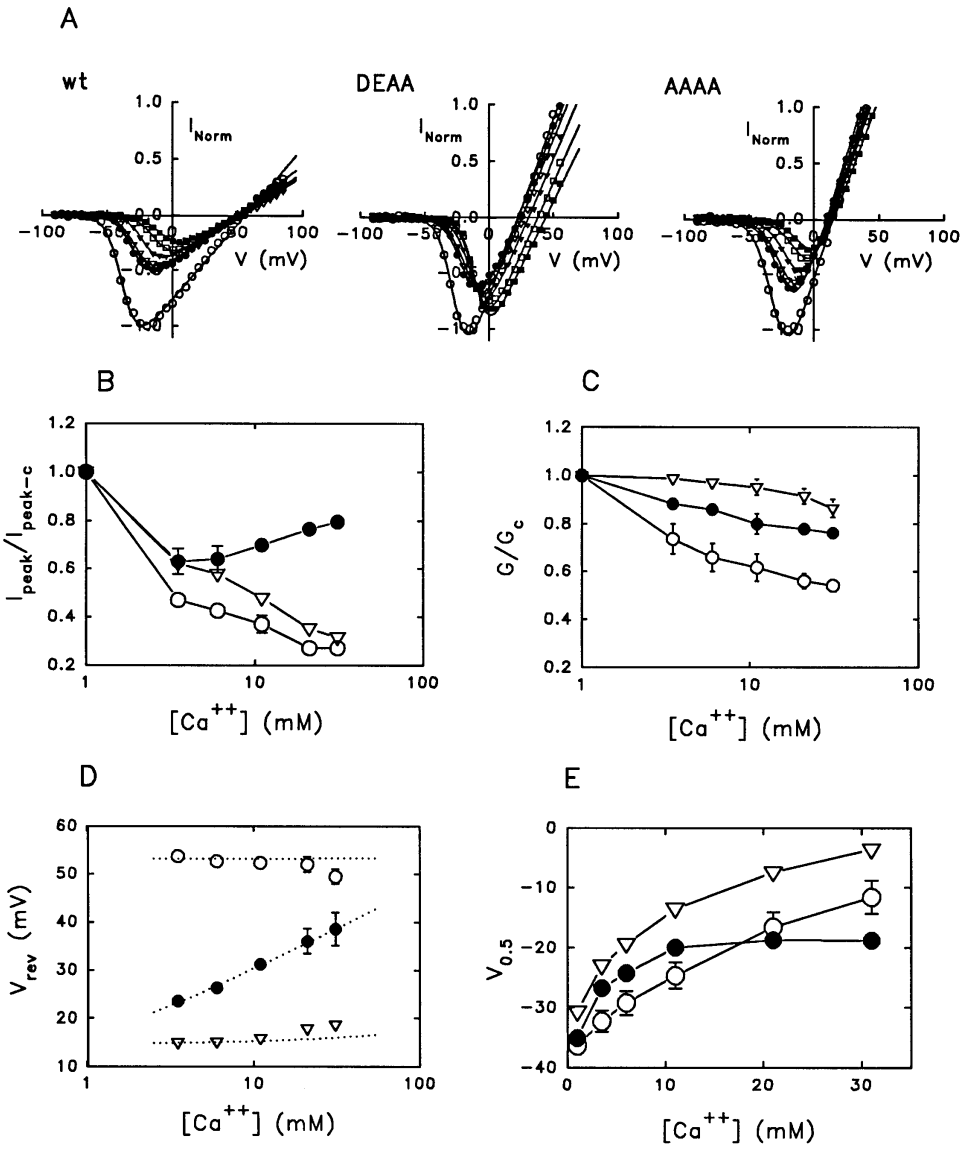

FIGURE 3. Effect of increasing extracellular Ca^{2+} on macroscopic current parameters in the presence of Na^+. (*A*) Normalized peak I–V relations and Boltzmann fits (*solid lines*) for HEK293 cells expressing wild-type, DEAA, or AAAA mutants. Points correspond to peak I–V data recorded in the presence of 140 mM NaCl plus 1 mM $CaCl_2$ (○), or 100 mM Na^+ plus the following mixtures of $CaCl_2$/Tris-Cl (mM): 3.5/37.5 (●), 6/35 (▽), 11/30 (▼), 21/20 (□), 31/10 (■). (*B*) Plot of the maximal peak current in the presence of increasing external Ca^{2+} normalized to that in the presence of 140 mM Na^+ plus 1 mM Ca^{2+}. (*C*) Plot of maximal macroscopic conductance (G_{max}) in the presence of increasing Ca^{2+} normalized to that in the presence of 140 mM Na^+ plus 1 mM Ca^{2+}. (*D*) Plot of the reversal potential (V_{rev}) in solutions containing 100 mM NaCl and increasing Ca^{2+}. (*E*) Plot of the measured $V_{0.5}$ parameter for voltage activation as a function of increasing Ca^{2+}. Symbols in *B–D* refer to wild-type (○), DEAA (●), and AAAA (▽) mutants. Data points and error bars in *B–E* correspond to the mean ± SD for four cells. Solid lines in *B, C,* and *E* connect the points and have no theoretical significance. The dotted lines in *D* are fits to the extended Goldman-Hodgkin-Katz equation (Lewis, 1979) using the following values for P_{Ca}/P_{Na}: 0.02, DEKA; 18.9, DEAA; 0.26, AAAA.

and this inhibition is reversed by increasing Ca^{2+} from 1 to 100 mM due to Ca^{2+} permeation (Heinemann et al., 1992; Schlief et al., 1996). Such behavior is reminiscent of native Ca^{2+} channels, where it has been interpreted on the basis of models assuming double occupancy of the channel by Ca^{2+} (Almers and McCleskey, 1984).

To investigate factors that may affect this phenomenon in the μ1 Na^+ channel, Fig. 3 *A* compares peak I–V data obtained in the presence of a control solution containing 140 mM NaCl plus 1 mM $CaCl_2$ with a series of solutions in which $CaCl_2$ is varied from 3.5 to 31 mM (in exchange for Tris-Cl at pH 7.3) at a constant 100 mM NaCl. In the case of the wild-type and AAAA channels, the reversal potential (V_R) does not change significantly with increasing [Ca^{2+}], as expected if Ca^{2+} is impermeant. In contrast, V_R shifts monotonically in the positive direction with increasing [Ca^{2+}] for the DEAA mutant (Fig. 3 *D*). The shift in V_R with increasing Ca^{2+} for DEAA can be fit by the Lewis equation (Lewis, 1979) using a value of P_{Ca}/P_{Na} = 18.9, which is similar to that calculated (Table I) from the Ca^{2+}-replacement experiments of Fig. 2. When maximal peak current is plotted as a function of [Ca^{2+}], the wild-type and AAAA channels exhibit simple inhibition, whereas the DEAA channel first exhibits a decrease in going from 1 to 3.5 mM Ca^{2+}, and then exhibits increasing peak current over the range of 3.5 to 31 mM Ca^{2+} (Fig. 3 *B*). One might be tempted to interpret this latter phenomenon as evidence of an "anomalous mole-fraction effect," but this is not warranted. Further analysis of the peak I–V relations (Fig. 3, *C–E*) shows that this behavior is a complex function of at least three effects: (*a*) an increased inward driving force ($V - V_R$) for the Ca^{2+}-permeable

DEAA mutant versus a constant driving force for wild type and AAAA (Fig. 3 *D*). (*b*) A differential effect of Ca^{2+} on the apparent maximal conductance as measured by G_{max} (Fig. 3 *C*). (*c*) A differential effect of Ca^{2+} on the midpoint voltage ($V_{0.5}$) for channel activation (Fig. 3 *E*). A true anomalous mole fraction effect is indicated by nonmonotonic behavior of the reversal potential or the unitary conductance with respect to mole-fraction mixtures of two permeant ions (Eisenman and Horn, 1983; Hille, 1992). Since the magnitude of the macroscopic peak current of Na^+ channels depends on the conductance, the reversal potential, and the voltage-activation range, this is not an appropriate parameter for evaluating this phenomenon.

Single-channel measurements have previously shown that extracellular Ca^{2+} produces a fast voltage-dependent block of wild-type Na^+ channels with an apparent K_D of ~35 mM and a voltage dependence equivalent to ~20–30% of the transmembrane electric field (Yamamoto et al., 1984; Nilius, 1988; Behrens et al., 1989; Ravindran et al., 1991). In macroscopic current records, this fast-blocking effect is most directly reflected by a reduction in the G_{max} parameter. The data of Fig. 3 *C* (G_{max} vs. $[Ca^{2+}]$) indicates that the blocking effect of Ca^{2+} is greatly reduced if not eliminated for the AAAA channel as compared with the DEKA wild type. For the DEAA mutant, the G_{max} data also shows weaker inhibition by Ca^{2+} relative to the wild type, but in this case Ca^{2+} itself carries significant current. Thus, G_{max} is not an appropriate measure of Ca^{2+} block by this mutant.

Another well-known action of external Ca^{2+} is to produce a positive shift in the voltage range of Na^+ channel activation (Frankenhaeuser and Hodgkin, 1957; Hille et al., 1975; Campbell and Hille, 1976; Cukierman et al., 1988). This phenomenon has been generally ascribed to screening and binding effects of Ca^{2+} on negative surface charges that influence the voltage-sensing mechanism (Hille, 1992). Fig. 3 *E* shows that Ala mutations of the DEKA locus cause significant changes in this property as indicated by the dependence of the $V_{0.5}$ parameter on external $[Ca^{2+}]$. Comparison of these data for the wild-type and AAAA channels shows that, over the range of $[Ca^{2+}]$ from 1 to 31 mM, both of these channels exhibit a +26-mV shift in $V_{0.5}$, but the $V_{0.5}$ data for the AAAA channel is displaced by +10 mV relative to wild type. This suggests that the AAAA channel has basically the same Ca^{2+} dependence as the wild type for this effect, except for a small systematic displacement. On the other hand, the $V_{0.5}$ data for the Ca^{2+}-permeable DEAA channel exhibits a different Ca^{2+} dependence than that of the wild-type or AAAA channels. Increasing $[Ca^{2+}]$ from 1 to 31 mM only produces a shift of +16 mV, with apparent saturation of $V_{0.5}$ at −20 mV. While we do not know the mechanism for this latter effect, it appears that the ability of Ca^{2+} to permeate through the DEAA channel has an influence on this gating shift behavior.

Blocking and Gating-shift Effect of External H^+

Na^+ channels are subject to modulation by external H^+ in a manner similar to the effects of external Ca^{2+} (Woodhull, 1973; Hille et al., 1975; Mozhayeva et al., 1981; Zhang and Siegelbaum, 1991; Hille, 1992; Daumas and Andersen, 1993). The mechanism of inhibition of macroscopic Na^+ current by low external pH has been attributed to at least two effects: (*a*) a fast, voltage-dependent block of the open channel caused by H^+ titration of one or more residues in the pore mouth. (*b*) A positive gating shift in the midpoint of voltage activation. To examine whether the charged residues of the DEKA locus play a role in these effects, we compared the current–voltage behavior of the DEKA, DEAA, and AAAA channels as a function of external pH. Fig. 4, *A–C* shows peak I–V relationships for these three channels in the range of pH 8.0–4.0. Parameters obtained from fitting these data to a Boltzmann function were used to grossly assess the blocking and gating-shift effect of H^+. The pH titrations of G_{max} relative to pH 7.3 are shown in Fig. 4 *D*. These data indicate that the AAAA channel is significantly more resistant to inhibition at low pH than the wild-type and DEAA channels. In contrast, the G_{max} titration curve of the DEAA mutant is only shifted to lower pH by ~0.2 pH units relative to the wild-type channel. The data in Fig. 4 *D* were fit to an empirical function: $G_{max}/G_{max,pH\ 7.3} = 1 - \{R_{max}/(1 + [H^+]_{0.5}/[H^+])\}$, where R_{max} is the maximal fraction of inhibited conductance and $[H^+]_{0.5}$ is the H^+ concentration at half-maximal inhibition. The respective values for R_{max} were: DEKA, 0.90 ± 0.02; DEAA, 0.86 ± 0.01; AAAA, 0.63 ± 0.02. Corresponding values obtained for $pH_{0.5}$ were: DEKA, 5.86 ± 0.04; DEAA, 5.62 ± 0.04; AAAA, 5.54 ± 0.06. These results indicate that the partial pH resistance of the AAAA mutant is due to an increase in the fractional conductance that is resistant to H^+ block and a small decrease in the apparent affinity for H^+. A similar comparison of the dependence of the midpoint for voltage activation, $V_{0.5}$, on $[H^+]$ shows that the three types of channels behave quite similarly in this respect (Fig. 4 *E*). This implies that the charged residues of the DEKA locus do not mediate the H^+-gating shift phenomenon.

Permeation of Organic Cations

The preceding characterization in HEK293 cells confirms that charged residues of the DEKA locus play a significant role in the process of ionic conduction as revealed by profound changes in selectivity for inorganic cations and secondary effects on the blocking action of external Ca^{2+} and H^+. The next question that we ad-

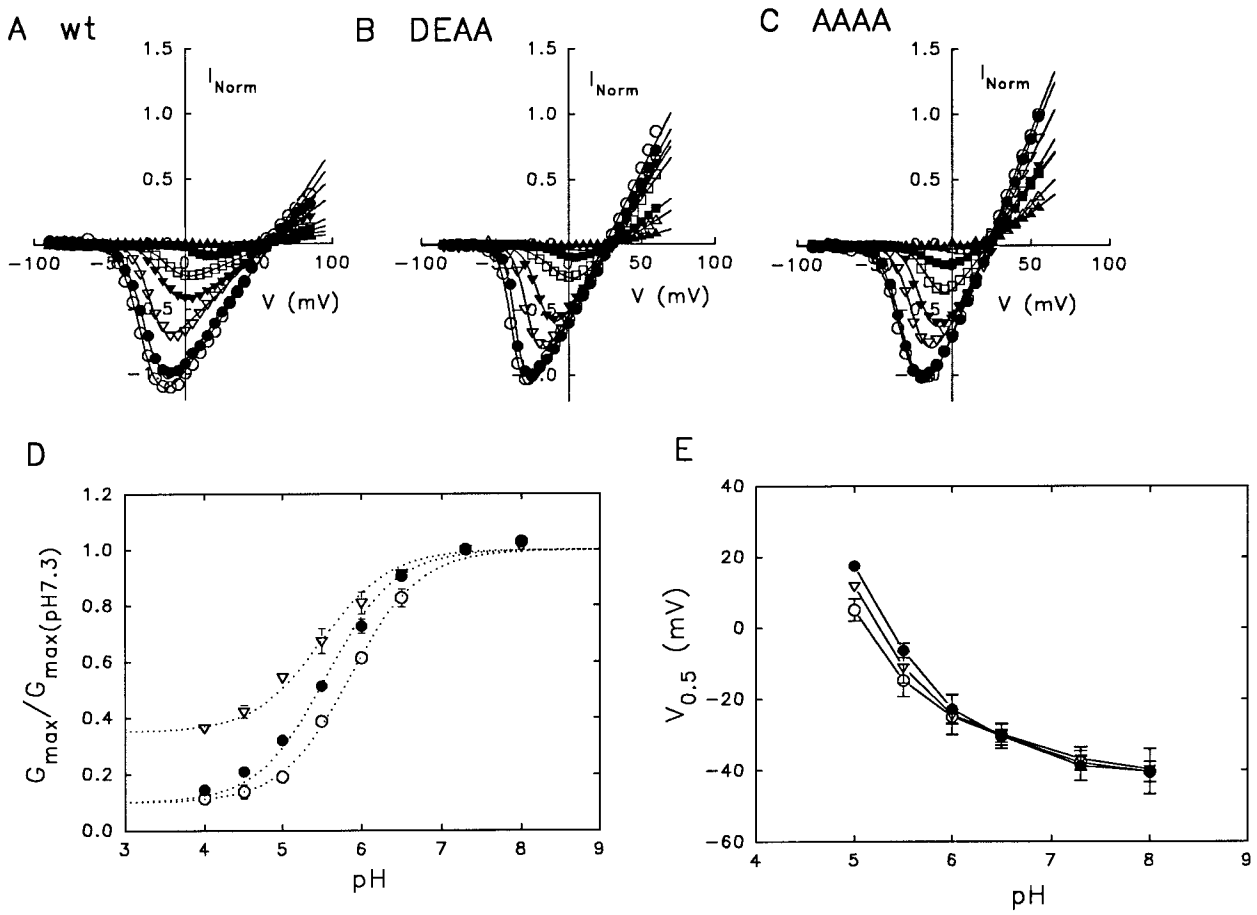

FIGURE 4. Effect of extracellular pH on macroscopic current parameters. (*A–C*) Peak I–V relations and Boltzmann fits (*solid lines*) for HEK293 cells expressing wild-type (*A*), DEAA (*B*), and AAAA (*C*) mutants in solutions containing 140 mM external Na^+ at the following pH values: 8.0 (○), 7.3 (●), 6.5 (▽), 6.0 (▼), 5.5 (□), 5.0 (■), 4.5 (△), 4.0 (▲). Current values are normalized to the peak current at pH 7.3. (*D*) Plot of maximal conductance (G_{max}) at various external pH values normalized to pH 7.3. Dotted lines are fit to the function, $G_{max}/G_{max,\,pH\,7.3} = 1 - \{R_{max}\,(1 + [H^+]_{0.5}/[H^+])\}$, as discussed in RESULTS. (*E*) Plot of the measured $V_{0.5}$ parameter for voltage activation as a function of external pH. Solid lines have no theoretical significance. Data points and error bars in *D* and *E* correspond to the mean ± SD for six to eight cells. Symbols in *D* and *E* refer to wild-type (○), DEAA (●), and AAA (▽) mutants.

dressed is whether mutations of the DEKA residues also influence the permeation of organic cations. Results of experiments examining the relative permeability of NH_4^+ and its four methyl derivatives are illustrated in Fig. 5. As expected from earlier studies (Hille, 1971; Campbell, 1976; Pappone, 1980), the wild-type μ1 channel is permeable to NH_4^+ ($P_X/P_{Na} = 0.33$), but is strictly impermeable to methyl, dimethyl, trimethyl, and tetramethylammonium ions (Fig. 5, Table II). In contrast, the DEAA mutant is permeable to all four of these ammonium derivatives (Fig. 5 *B*). Typical voltage-activated inward currents recorded in the presence of 140 mM NH_4^+, methylamine (MA), or TMA for cells expressing the DEAA channel are illustrated in Fig. 5 *A*. Analysis of the peak I–V relationships for this mutant (Fig. 5 *B*) leads to a curious observation. On the basis of the measured reversal potentials and current magnitudes (Table II), TMA ($P_X/P_{Na} = 0.50 \pm 0.04$) is slightly more permeable than MA ($P_X/P_{Na} = 0.41 \pm 0.04$); however, the relative peak current carried by MA ($I_X/I_{Na} = 0.32 \pm 0.04$) is larger than that of TMA ($I_X/I_{Na} = 0.18 \pm 0.01$). When the relative permeability or maximal peak current for the DEAA mutant is plotted as a function of molecular volume of the methylated ammonium cations (Fig. 6), these plots appear to exhibit a minimum at dimethylamine (DMA) or trimethylamine (TriMA). Considering that TMA (minimum diameter = 6.0 Å, vol = 78.8 $Å^3$) is substantially larger than MA (minimum diameter = 3.8 Å, vol = 35.1 $Å^3$), this comparison indicates that the relative permeability of organic cations through the DEAA channel is not inversely related to the size of these molecules in a simple fashion.

Similar characterization of the other Ala mutations, DAAA, AEAA, and AAAA, revealed that substitution of Ala for the Asp(I) and Glu(II) residues further dimin-

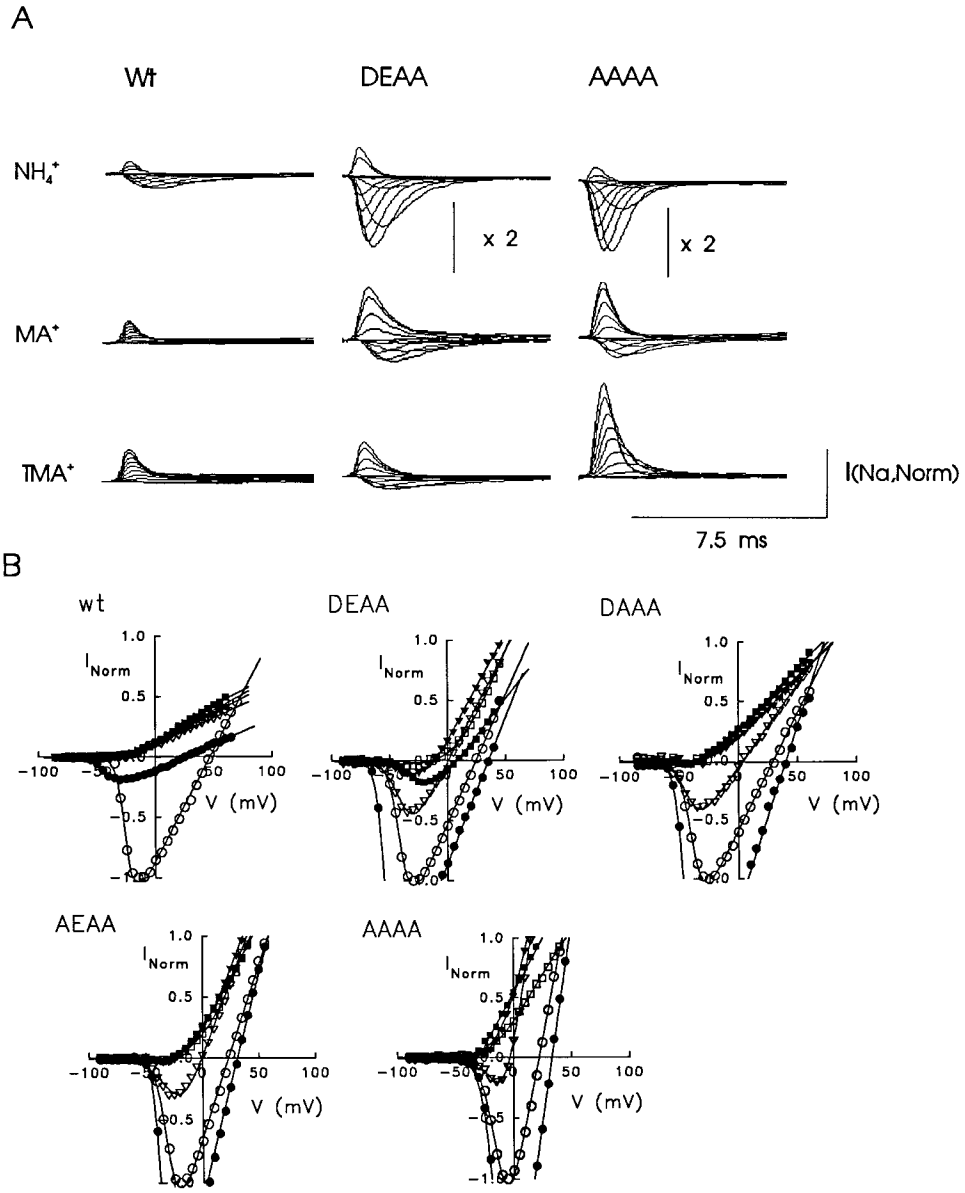

FIGURE 5. Comparison of the permeation behavior of ammonium and methylated ammonium derivatives in wild-type and mutant Na^+ channels. (*A*) Typical currents recorded in the presence of extracellular NH_4^+, MA, and TMA for wild-type, DEAA, and AAAA mutants. Currents were activated by step depolarization from a holding voltage of −120 mV to voltages ranging from −90 to +60 mV in steps of 10 mV. Currents are normalized to the peak Na^+ current from the same cell corresponding to the 1× vertical scale bar. NH_4^+ currents for DEAA and AAAA are shown at half scale. (*B*) Normalized peak I–V relations for typical cells expressing wild-type, DEAA, DAAA, AEAA, or AAAA mutants. Solid line curves indicate fits to a Boltzmann function (Eq. 1). I–V relations recorded in the following cation solutions (140 mM Cl^- salts) are superimposed: Na^+ (○), NH_4^+ (●), MA (▽), DMA (▼), TriMA (□), and TMA (■).

ishes the permeability of methylated ammonium cations observed in the DEAA background. For example, Fig. 5 *A* shows that MA carries current through the AAAA channel but TMA does not. In general, the results of Fig. 5 and Table II indicate that MA is the only methylated derivative of ammonium that readily permeates through the DAAA, AEAA, and AAAA channels. Close inspection of the I–V data for the AEAA mutant reveals a rightward shift of the I–V curves relative to that of AAAA, which suggest that DMA, TriMA, and TMA are slightly permeant in AEAA; but, if so, these cations carry very little inward current (Table II). Taken together, these results demonstrate that the single-mutation substitution of Lys(III) by Ala causes a dramatic increase in permeability to MA, DMA, TriMA, and TMA. However, this enhanced permeability to organic cations in DEAA is partially reversed by Ala substitution of the Asp(I) and Glu(II) residues to produce the AAAA mutant (Table II). Since the carboxylate functional groups of Asp and Glu are physically larger than the methyl group of Ala, this indicates that the molecular cutoff behavior of these mutant Na^+ channels is not simply specified by the combined side chain volume of the Asp(I), Glu(II), and Lys(III) residues. Rather, when Lys(III) is replaced by Ala, it appears that the Asp(I) and Glu(II) residues actually cooperate to facilitate the permeation of large organic cations.

This conclusion is further strengthened by experiments of Fig. 7, which examine the permeability of wild-type, DEAA, and AAAA channels to the following

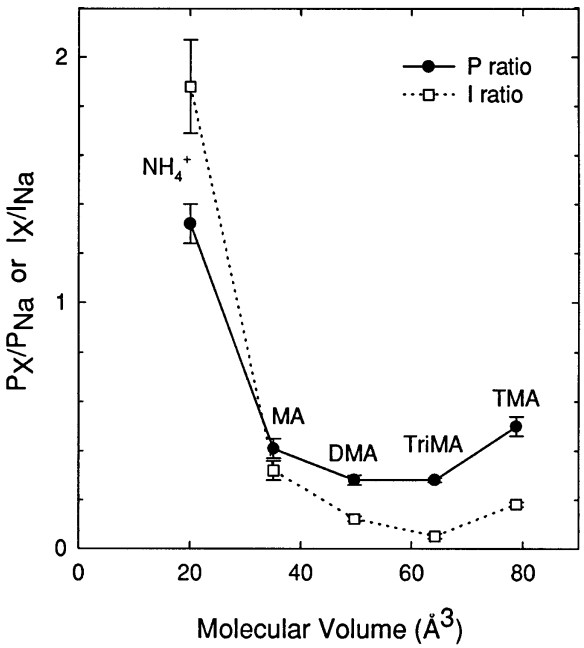

FIGURE 6. Anomalous molecular sieving behavior of the DEAA mutant. Maximal peak current relative to Na^+ (□) and relative permeability (●) for the series NH_4^+, MA, DMA, TriMA, and TMA are plotted versus molecular volume of the cation as measured using Insight software.

organic cations: ethylamine (EA), ethanolamine (EAOH), choline, TEA, and Tris. As expected, the wild-type channel is impermeable to all of these cations. In contrast, both DEAA and AAAA exhibit small but detectable inward currents in the presence of extracellular EA, which corresponds to a permeability ratio of ~0.35 for this organic cation relative to Na^+ (Table II). This is analogous to the permeability behavior of MA described above in reference to the experiments of Fig. 5. The DEAA channel is also permeable to each of the other large cations of this series, including TEA. However, the wild-type and AAAA channels are not permeable to these other large cations (Fig. 7, Table II). This behavior is also quite similar to that outlined above for the DEAA and AAAA mutants with respect to the methylated ammonium derivatives. In terms of relative permeability to the various large organic cations that range in molecular volume from 49.4 Å^3 for EA to 136.9 Å^3 for TEA, it appears that the DEAA channel is not very discriminating (Table II, see Fig. 10, *A* and *B*). For example, EA, EAOH, choline, and TEA exhibit a similar peak current magnitude in the range of 0.11–0.14 of the peak Na^+ current. The calculated relative permeabilities of these latter four cations for the DEAA mutant are also rather similar, ranging from 0.26 ± 0.04 for TEA to 0.46 ± 0.02 for EAOH (Table II). The Tris cation is somewhat of an exception with a distinctly lower permeability ratio of 0.19 ± 0.04 and a barely detectable inward current (Fig. 7 *B*, Table II). To summarize, these results again suggest that molecular size of the DEKA residues and that of the test cations are not the only factors that determine the relative permeability of organic cations in these mutants.

Hille (1971, 1992) has suggested that the permeability of the relatively large guanidinium molecule through the native Na^+ channel is related to the ability of this organic cation to serve as a hydrogen bond donor to oxygen atoms that line the selectivity filter. To explore this idea in the present context, we measured the relative permeability of the following molecules: guanidine, aminoguanidine, methylguanidine, and hydroxylamine for the wild-type, DEAA, and AAAA mutants. The results indicate that the relative permeability for guanidine is increased from 0.19 ± 0.04 in the wild-type DEKA channel to 0.91 ± 0.29 for the DEAA mutant. This is accompanied by an approximately sixfold increase in the peak guanidinium current relative to Na^+ (Table II). However, neutralization of the Asp(I) and Glu(II) residues to Ala in the AAAA mutant caused little change in guanidine permeability as compared with DEAA (Fig. 8, Table II). Since the all-methyl form of the DEKA locus in the AAAA mutant cannot participate in hydrogen bond formation via its functional groups, one would have expected the relative permeability of guanidine to fall considerably in this mutant; however, this was not observed. For Na^+ channels studied in myelinated nerve fibers, aminoguanidine and hydroxylguanidine were the largest cations found to be barely permeable (Hille, 1971). We did not detect inward current carried by aminoguanidine through the wild-type rat muscle channel in our experiments, but this molecule does appear to be permeable in the DEAA mutant (P_X/P_{Na} = 0.28). Methylguanidine is an interesting case, since it provides an example of an organic cation that does not conduct inward current through either the wild-type, DEAA, or AAAA mutants. The ammonium derivative, hydroxylamine, with a pKa of 5.95, is also a unique probe of the conduction pathway since it is the only nonmetal ion that is just as permeable as Na^+ and Li^+ in native Na^+ channels (Hille, 1971; Campbell, 1976; Pappone, 1980). In our experiments, hydroxylammonium (measured at pH 6.0 since its pKa is 5.9) also had the highest permeability among all of the tested monovalent cations. Its relative permeability was found to increase by factors of 1.6 and 1.4 over wild type in the DEAA and AAAA mutants, respectively (Fig. 8, Table II). As a control experiment, Fig. 8 *B* shows that the reversal potential measured in the presence of hydroxylamine undergoes a large positive shift as the pH is changed from 7.3 to 6.0, as expected for protonation of the neutral form of hydroxylamine.

TABLE II

Selectivity Properties of Wild-Type and Mutant Na^+ Channels for Organic Cations

Cation	Dia*	Vol‡	Parameter	DEKA (wt)	DEAA	DAAA	AEAA	AAAA
	Å	*Å*^{3}						
NH_4^+	3.6	20.1	V_R	23.0 ± 3.5 (4)	29.3 ± 1.0 (5)	38.8 ± 2.2 (3)	31.4 ± 2.6 (3)	34.8 ± 1.8 (4)
			P/P_{Na}	0.33 ± 0.10	1.32 ± 0.08	1.53 ± 0.09	1.43 ± 0.04	1.61 ± 0.05
			I/I_{Na}	0.18 ± 0.01	1.88 ± 0.19	2.18 ± 0.07	1.80 ± 0.01	2.04 ± 0.02
MA	3.8	35.1	V_R	<−30.0 ± 4.1 (4)	−0.28 ± 0.15 (3)	3.0 ± 4.5 (3)	−1.9 ± 1.2 (3)	−0.2 ± 2.3 (3)
			P/P_{Na}	<0.05	0.41 ± 0.04	0.37 ± 0.02	0.43 ± 0.02	0.41 ± 0.03
			I/I_{Na}	<0.01	0.32 ± 0.04	0.37 ± 0.01	0.29 ± 0.01	0.26 ± 0.06
DMA	4.6	49.7	V_R	<−30.1 ± 5.8(3)	−9.9 ± 0.4 (3)	<−37.9 ± 3.9(3)	<−25.3 ± 3.7(3)	<−40.1 ± 2.1(3)
			P/P_{Na}	<0.05	0.28 ± 0.02	<0.07	<0.16	<0.08
			I/I_{Na}	<0.01	0.12 ± 0.01	<0.01	<0.01	<0.01
TriMA	6.0	64.2	V_R	<−25.9 ± 3.6(3)	−10.6 ± 1.8 (4)	<−35.5 ± 6.3(3)	<−29.2 ± 3.3(3)	<−41.8 ± 2.5(3)
			P/P_{Na}	<0.07	0.28 ± 0.01	<0.08	<0.15	<0.08
			I/I_{Na}	<0.01	0.05 ± 0.01	<0.01	<0.01	<0.01
TMA	6.0	78.8	V_R	<−34.4 ± 4.0(3)	3.7 ± 0.3 (4)	<−35.3 ± 7.7(3)	<−31.7 ± 1.9(2)	<−45.0 ± 3.5(3)
			P/P_{Na}	<0.05	0.50 ± 0.04	<0.08	<0.12	<0.07
			I/I_{Na}	<0.01	0.18 ± 0.01	<0.01	<0.01	<0.01
EA	4.6	49.4	V_R	<52.7 ± 3.2(3)	−5.6 ± 2.9 (3)	—	—	−2.2 ± 2.7 (4)
			P/P_{Na}	<0.01	0.34 ± 0.04	—	—	0.36 ± 0.05
			I/I_{Na}	<0.01	0.11 ± 0.01	—	—	0.08 ± 0.02
EAOH	4.6	56.5	V_R	<−25.0 ± 6.4(3)	1.8 ± 1.6 (3)	—	—	<−33.5 ± 1.6(3)
			P/P_{Na}	<0.03	0.46 ± 0.02	—	—	<0.10
			I/I_{Na}	<0.01	0.14 ± 0.01	—	—	<0.01
Choline	6.0	100.6	V_R	<−35.5 ± 6.2(3)	−10.4 ± 1.9 (3)	—	—	<−43.8 ± 3.1(3)
			P/P_{Na}	<0.03	0.32 ± 0.04	—	—	<0.07
			I/I_{Na}	<0.01	0.11 ± 0.01	—	—	<0.01
TEA	8.2	136.9	V_R	<−42.9 ± 6.4(3)	−15.7 ± 1.1 (3)	—	—	<−48.1 ± 3.6(3)
			P/P_{Na}	<0.02	0.26 ± 0.03	—	—	<0.06
			I/I_{Na}	<0.01	0.13 ± 0.01	—	—	<0.01
Tris	6.8	98.6	V_R	<−42.4 ± 6.4(3)	−18.2 ± 7.8 (4)	—	—	<−47.3 ± 2.5(3)
			P/P_{Na}	<0.02	0.19 ± 0.04	—	—	<0.06
			I/I_{Na}	<0.01	0.02 ± 0.01	—	—	<0.01
Guanidine	5.8	49.1	V_R	10.8 ± 2.4(3)	22.8 ± 3.2 (5)	—	—	23.8 ± 3.5 (4)
			P/P_{Na}	0.19 ± 0.04	0.91 ± 0.29	—	—	0.97 ± 0.11
			I/I_{Na}	0.06 ± 0.01	0.38 ± 0.01	—	—	0.36 ± 0.02
Aminoguanidine	5.8	58.3	V_R	<−43.8 ± 6.6(3)	−12.4 ± 2.5 (3)	—	—	<−42.9 ± 1.9(3)
			P/P_{Na}	<0.02	0.28 ± 0.02	—	—	<0.08
			I/I_{Na}	<0.01	0.05 ± 0.01	—	—	<0.01
Methylguanidine	5.8	63.7	V_R	<−57.9 ± 3.8(3)	<−54.8 ± 2.0(3)	—	—	<−54.3 ± 1.6(3)
			P/P_{Na}	<0.01	<0.04	—	—	<0.05
			I/I_{Na}	<0.01	<0.01	—	—	<0.01
NH_3OH^+ (pH 6.0)	3.8	27.0	V_R	47.7 ± 3.4 (3)	37.8 ± 4.2 (3)	—	—	43.9 ± 4.4 (3)
			P/P_{Na}	1.78 ± 0.07	2.94 ± 0.02	—	—	2.55 ± 0.11
			I/I_{Na}	0.29 ± 0.04	1.19 ± 0.14	—	—	1.11 ± 0.15

Selectivity parameters are described in the notes to Table I. *Diameter measurement corresponds to the minimum diameter of a circle that fully encloses a molecular model of the cation in its narrowest orientation as determined with the Select Sphere option of Hyperchem software. ‡Volume measurement corresponds to the van der Waals volume enclosed by a space-filling model of the molecule as calculated by Insight software.

Toxin Sensitivity

The preceding results indicate that there is a large change in molecular sieving behavior when the Lys(III) residue is mutated to Ala. Since the native DEKA channel is impermeable to MA (minimum diameter = 3.8 Å) and the DEAA mutant is permeable to cations as large as TEA (minimum diameter = 8.2 Å), it appears that the effective pore diameter has increased by at least twofold as a result of this mutation. Despite the fact that Ala mutations of the DEKA locus exhibit rather normal gating behavior, this large increase in apparent pore diameter raises the question of whether

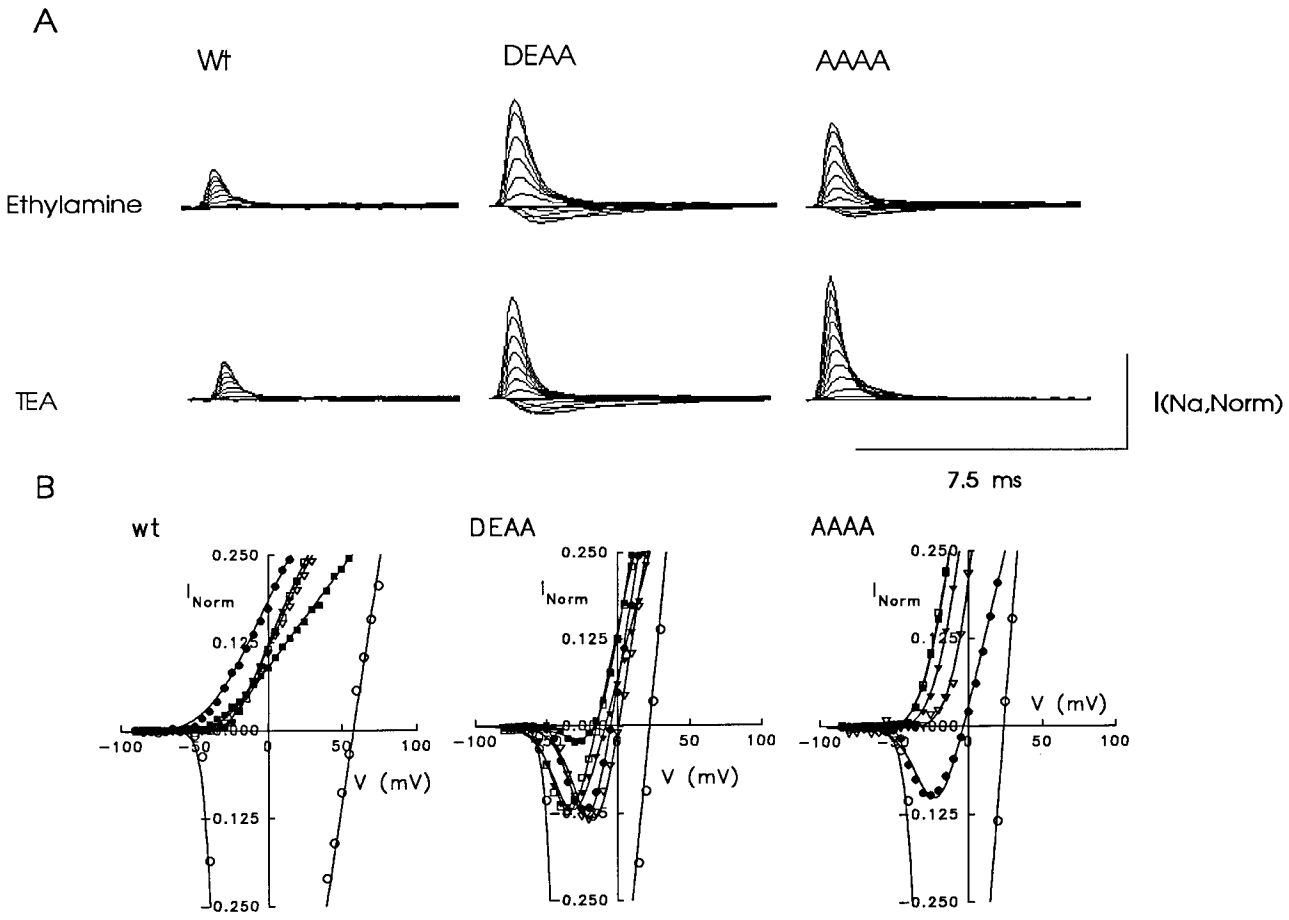

FIGURE 7. Comparison of the permeation behavior of large organic cations in wild-type and mutant Na^+ channels. (*A*) Typical currents recorded in the presence of extracellular EA and TEA for wild-type, DEAA, and AAAA mutants. Currents were activated by the same voltage protocol described in Fig. 5. The vertical calibration corresponds to the normalized peak Na^+ current. (*B*) Normalized peak I–V relations and Boltzmann fits (*solid lines*) for typical cells expressing wild-type, DEAA, or AAAA mutants. I–V relations recorded in Na^+ or the following organic cation solutions (140 mM) are superimposed: Na^+ (○), EA (●), EAOH (▽), choline (▼), TEA (□), and Tris (■). The normalized current scale is truncated to enlarge results for organic cations.

these mutations may cause extensive structural changes in the channel protein. In an attempt to address this question, we measured the blocking affinity of the DEAA and AAAA mutants for the small guanidinium toxins, tetrodotoxin (TTX) and saxitoxin (STX), and the peptide toxin, μ-conotoxin GIIIB. As the focus of many previous investigations, the latter toxins are now generally assumed to competitively bind in the outer vestibule and block Na^+ channels by directly occluding the entrance to the pore. Indeed, Terlau et al. (1991) previously showed that several mutations of the DEKA locus and adjacent P-region residues in domains I–IV cause large changes in affinity for the low molecular weight guanidinium toxins, TTX (M_r = 319) and STX (M_r = 299). Similarly, we find that the DEAA mutant has ~430-fold lower affinity for block by TTX and ~720-fold lower affinity for block by STX than that of the native channel, and the AAAA mutant is practically insensitive to block by 10 μM TTX and STX (Fig. 9 *A*).

In contrast, sensitivity to block by the 22-residue peptide, GIIIB (M_r = 2,640), is not as strongly affected by these mutations. The apparent affinity for GIIIB of the DEAA and AAAA mutants is, respectively, only ~3.4- and ~11.7-fold lower than that of the native channel (Fig. 9 *A*). This loss in affinity is primarily reflected in faster dissociation rates of GIIIB as measured after washout (Fig. 9 *B*). The closely related μ-conotoxin, GIIIA, is known to have a starlike, discoidal solution structure with a diameter of roughly 20–25 Å (Lancelin et al., 1991). Structure–activity studies from several laboratories indicate that the total binding energy of this molecule to the rat muscle Na^+ channel is derived from numerous weak molecular interactions with channel residues that line the outer vestibule (Sato et al., 1991; Becker et al., 1992; Chanine et al., 1995; Dudley et al., 1995). If the Ala mutations that we have studied cause a major structural rearrangement of the channel protein as manifested by a large increase in pore diameter, we

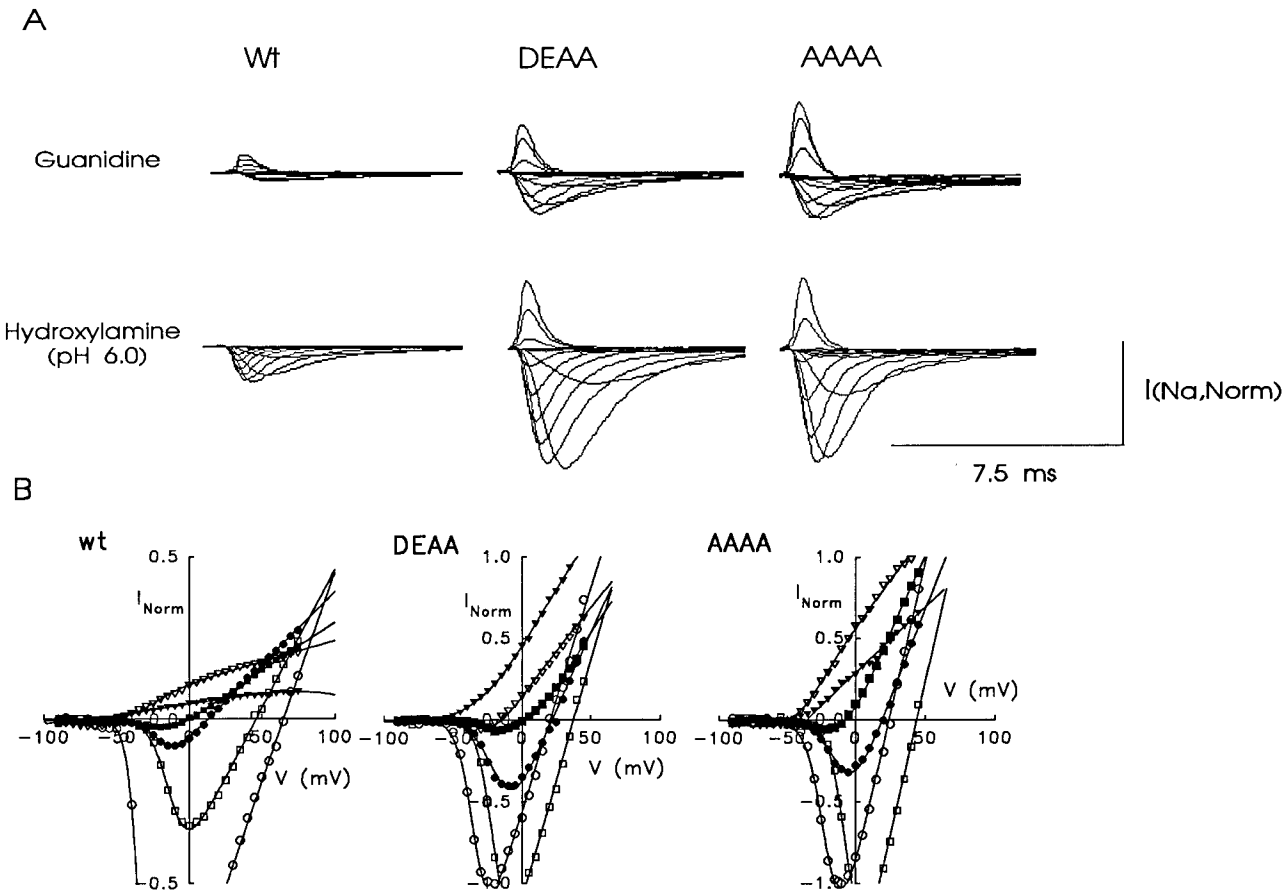

FIGURE 8. Comparison of the permeability behavior of guanidinium cations and hydroxylammonium in wild-type and mutant Na^+ channels. (*A*) Typical currents recorded in the presence of extracellular guanidine and hydroxylamine (at pH 6.0) for wild-type, DEAA, and AAAA mutants. Currents were activated by the same voltage protocol described in Fig. 5. The vertical calibration is 1× for normalized peak Na^+ current. (*B*) Normalized peak I–V relations and Boltzmann fits (*solid lines*) for typical cells expressing wild-type, DEAA, or AAAA mutants. I–V relations recorded in Na^+ or the following organic cation solutions (140 mM) are superimposed: Na^+ (○), guanidine (●), aminoguanidine (▽), methylguanidine (▼), hydroxylamine at pH 6.9 (□), and hydroxylamine at pH 7.3 (■). The normalized current scale is truncated for the wild type.

would have expected to observe virtual destruction of the vestibule binding site for GIIIB. The fact that the μ-conotoxin binding site is clearly intact in the DEAA and AAAA mutants is consistent with the idea that these mutations cause only small structural changes in the vicinity of the DEKA residues.

DISCUSSION

The major conclusion that emerges from this work is that charged residues of the DEKA locus are important structural determinants of the molecular sieving behavior of the μ1 Na^+ channel. The effect on organic cation permeation reported here is not merely a subtle perturbation of relative permeability. Rather, mutation of Lys(III) to Ala makes the Na^+ channel permeable to a whole class of large organic cations that normally do not carry current through the wild-type channel. This gain of function observed for the DEAA mutant (Figs. 5 and 7) is accompanied by the loss of selectivity for alkali cations (Fig. 1) and the gain of permeability for Ca^{2+} and other group IIA divalent cations (Fig. 2), as first discovered by Heinemann et al. (1992) for the DEEA mutation of the rat brain II Na^+ channel. These findings are summarized by the following minimal list of substrate specificity functions that may be associated with residues of the DEKA locus: (*a*) Ca^{2+} exclusion, (*b*) Na^+/K^+ discrimination, and (*c*) organic cation exclusion.

The present results further enhance the view that the DEKA/EEEE loci of Na^+/Ca^{2+} channels primarily account for key functional differences in the substrate specificity properties of these two homologous channel proteins. The Lys(III) Ala mutant is characterized by a high value for P_{Ca}/P_{Na}, relative nonselectivity among monovalent inorganic cations, and permeability for large organic cations in the absence of Ca^{2+}. These latter features are also basic characteristics of Ca^{2+} channels (Almers et al., 1984; McCleskey and Almers, 1985).

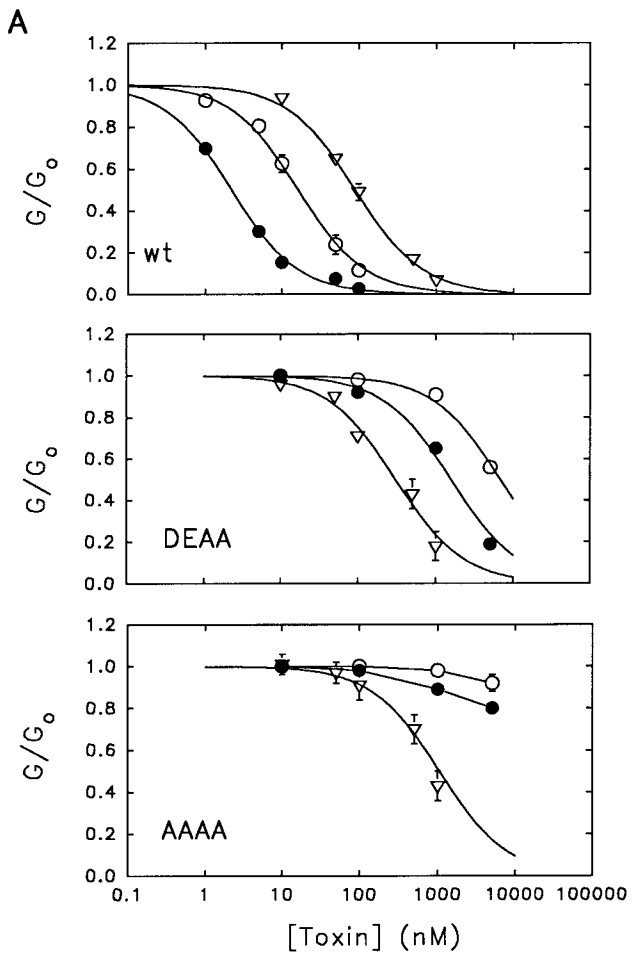

C K_I values

	wt (DEKA)	DEAA	AAAA
TTX	16.71±1.11 (nM)	6.82±0.61 (μM)	57.04±1.44 (μM)
STX	2.18±1.41 (nM)	1.56±0.19 (μM)	18.01±0.34 (μM)
μ-conotoxin	96.71±5.11 (nM)	0.30±0.04 (μM)	0.93±0.10 (μM)

FIGURE 9. Comparison of the sensitivity to various toxins. (*A*) Titration curves for inhibition of Na^+ current by TTX (○), STX (●), and μ-conotoxin GIIIB (▽) for the wild-type, DEAA, and AAAA mutants. Symbols are the mean ± SEM for three determinations. The ordinate axis is the G_{max} obtained from Boltzmann fitting of the peak I–V relation normalized to that measured in the absence of toxin. Solid lines indicate fits to a one-site inhibition curve: $G/G_0 = K_I/(K_I + [\text{toxin}])$ with the values for K_I given in *C*. (*B*) Kinetics of μ-conotoxin GIIIB action for wild-type, DEAA, and AAAA mutants. Voltage-clamped cells were depolarized to +30 mV from a holding voltage of −120 mV at a frequency of 1/30 Hz. Relative conductance at the peak inward current before toxin addition is normalized to 1.0 for each case. The two vertical dotted lines indicate onset of perfusion with toxin-containing solution (1 μM GIIIB) and replacement by toxin-free solution. Data points corresponding to toxin dissociation are fit to a single exponential function with the following rate constants: $2.38 \times 10^{-4}\ s^{-1}$, DEKA; $1.61 \times 10^{-3}\ s^{-1}$, DEAA; $1.38 \times 10^{-2}\ s^{-1}$, AAAA.

Thus, the current findings for organic cations are qualitatively consistent with behavior that would be expected for functional conversion of a Na^+ channel to a Ca^{2+} channel. To be sure, there are specific quantitative differences, but the relative permeability ratios of organic cations for the DEAA mutant (Table II, Fig. 10 *A*) are similar to analogous data for the frog skeletal muscle Ca^{2+} channel measured in the absence of Ca^{2+} (McCleskey and Almers, 1985). This supports the idea proposed in our last study (Favre et al., 1996) that the alkyl-ammonium group of Lys(III) essentially functions as a molecular sentry in the Na^+ channel by denying entrance to unauthorized cations (Ca^{2+}, Mg^{2+}, large organic cations) and controlling the ratio of desirable (Na^+) to undesirable (K^+) monovalent cations that are allowed to pass through the pore. These data also add weight to the notion that the Lys(III) residue is functionally analogous to the Ca^{2+} ion that occupies a high affinity binding site in the Ca^{2+} channel pore under physiological conditions. According to current theory (Sather et al., 1994), this bound Ca^{2+} ion in the Ca^{2+} channel controls selectivity for inorganic cations, and it also apparently prevents the permeation of large organic cations, two functions that are analogous to those identified here for the Lys(III) residue of the Na^+ channel.

Permeation of Organic Cations in Alanine Mutants of the DEKA Locus

According to the model proposed by Hille (1971, 1992), the selectivity filter is a specific region of the

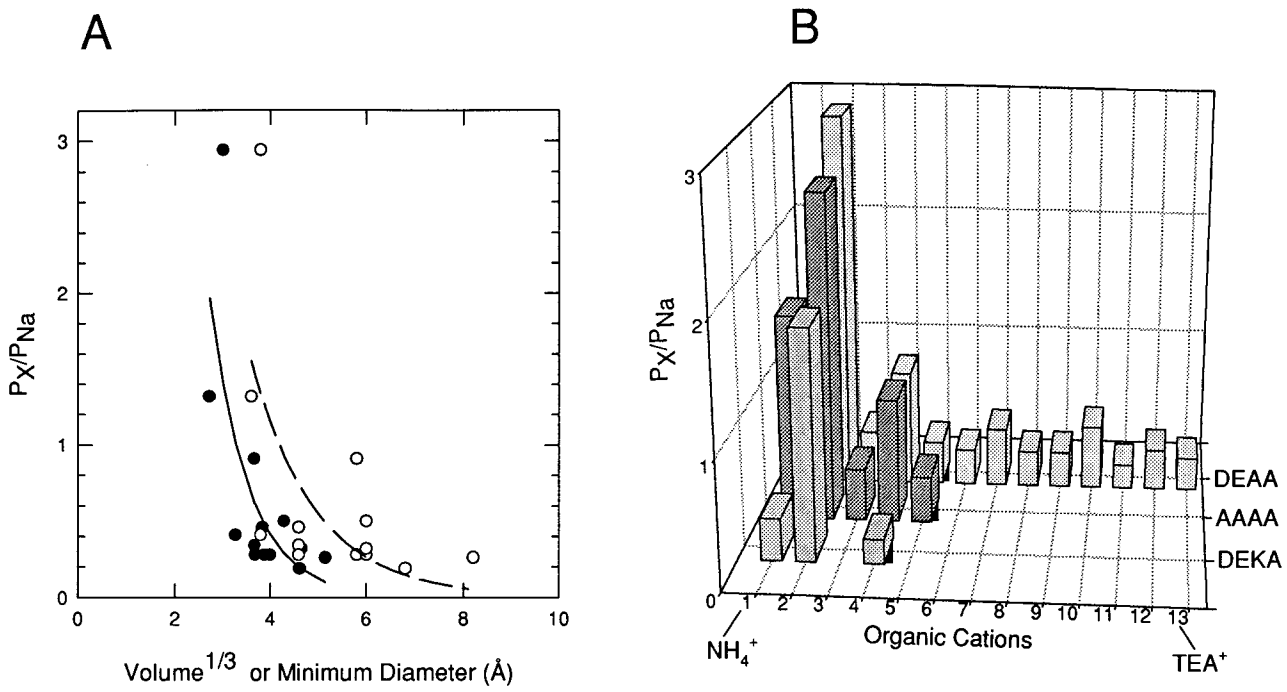

FIGURE 10. Graphical summary of major results for organic cations. (*A*) P_X/P_{Na} values listed in Table II for organic cations permeable through the DEAA mutant are plotted versus the cube root of molecular volume of the cation (●) or versus the minimum diameter of the cation (○). Minimum diameter is defined by the diameter of a circle that can completely enclose a space-filling representation of the molecule in its narrowest orientation. To indicate the general trend of the data, points for the two different methods of comparing molecular size are fit to a single exponential function as indicated by the solid and dashed lines. (*B*) Bar graph illustrating the increase in relative permeability (P_X/P_{Na}) for small cations and acquisition of new permeability to large cations for AAAA and DEAA mutants as compared with wild type. The axis labeled Organic Cations is numbered from 1–13, denoting permeant cations of Table II in order of increasing molecular volume as follows: NH_4^+ (*1*), NH_3OH^+ (*2*), MA (*3*), guanidine (*4*), EA (*5*), DMA (*6*), EAOH (*7*), aminoguanidine (*8*), TriMA (*9*), TMA (*10*), Tris (*11*), choline (*12*), TEA (*13*).

Na^+ channel pore that directly interacts with inorganic ions and discriminates among them on the basis of their size, charge, and dehydration energy. It was also proposed that this filter determines which organic cations permeate through the channel at a rate large enough to carry measurable current. In Hille's model, the molecular cutoff for permeation of large organic cations arises from the relatively rigid physical barrier formed by the atoms of Na^+ channel residues that surround this filter region and from the ability of some molecules (such as guanidine) to preferentially squeeze through this narrow constriction by forming hydrogen bonds with oxygen atoms of the filter. Organic cations with methyl groups and larger alkyl substituent groups were thought to be impermeant because their physical dimensions are too wide and their molecular surfaces are too hydrophobic to permit rapid passage through the relatively more polar selectivity filter. Thus, if the residues of the DEKA locus actually form the lining of such a constricted hole or filter region, one would predict that substitution of these residues by amino acids with smaller side chains such as Ala would widen this hole and allow permeation of larger organic cations. Substitution of Lys(III) by Ala clearly removes a major barrier to the permeation of large organic cations, as expected for such a selectivity filter. However, the detailed behavior of the mutations that we have characterized does not entirely correspond to the conventional idea of molecular sieving, in the sense of a chemically inert pore that selects purely on the basis of size.

Simple molecular sieving by an ion channel protein is exemplified by the acetylcholine receptor. For this channel, the relative permeability of many organic cations follows a well-defined inverse relationship with respect to a basic measure of size such as the molecular weight of the permeant cations (e.g., Fig. 5 *A* of Dwyer at al., 1980). For several theories of molecular filtration through a cylinder based purely on mechanical sieving, permeability is expected to decrease to zero according to the term $(1 - a/r)^2$, where a is the radius of permeating spheres and r is the cylinder radius (Dwyer et al., 1980). By this relationship, the acetylcholine receptor exhibits an apparent diameter of ~6.5 Å based on data for the relative permeability of 70 different cations (Dwyer et al., 1980; Dwyer and Farley, 1984; Wang and Imoto, 1992). This observation led Hille and co-workers to conclude that the size of the ion is the major determinant of permeability in this receptor channel

(Dwyer et al., 1980). Such behavior was also found for the Ca^{2+} channel in the absence of Ca^{2+} (Fig. 4 of McCleskey and Almers, 1985). In the present work on the μ1 Na^+ channel, the data of Fig. 10 *A* for the DEAA mutant are roughly consistent with a molecular sieving phenomenon, since large molecules tend to exhibit a generally lower permeability than small molecules.

In evaluating such relationships, there is an inherent uncertainty in comparing molecules with different shapes. Dwyer et al. (1980) treated this problem by defining mean molecular diameter as the geometric mean of the three dimensions of a rectangular box that would contain the molecule. The data of Fig. 10 *A* for the DEAA mutant are plotted to compare two different methods of size comparison: the cube root of van der Waals volume and the minimum diameter of a hole through which the molecule can pass in its narrowest orientation. This plot indicates that the shape-insensitive, $Volume^{1/3}$ parameter exhibits a tighter correlation with relative permeability than Minimum Diameter, which reflects differences in molecular shape. This plot does show an inverse relationship between permeability and size, but based on the observed scatter, the correlation is not as well defined as that for the acetylcholine receptor. For example, a log–log plot of P_X/P_{Na} vs. $Volume^{1/3}$ has a correlation coefficient of $r = -0.74$ by linear regression analysis (not shown). The scatter in this data might partly reflect the fact that we have not sampled enough differently sized molecules to empirically define an underlying sieving relationship. But it might also indicate that this system is subject to many specific deviations from simple mechanical sieving theory.

As noted in RESULTS, a clear violation of sieving behavior is the data of Fig. 6, which shows the relative permeability of a subset of ammonium cations, NH_4^+, MA, DMA, TriMA, and TMA, for the DEAA mutant. This regular molecular series is a good test of sieving behavior since the five molecules have the same basic geometry and differ only by the substitution of methyl groups for hydrogen atoms. A pure sieving model would predict that permeability should decrease in a monotonic fashion with molecular size or volume. In contrast, the data of Fig. 6 is anomalous since the largest cation of this regular ammonium series, TMA, seems to be as permeant as MA, whereas DMA and TriMA are less permeant. Another example of the violation of simple sieving behavior is the large cation, TEA, which has approximately the same relative permeability (0.26 ± 0.03) as DMA (Table II). Such anomalies suggest that the type of molecular sieving encountered in the DEAA mutant is influenced by a component involving chemical selection. What factors could explain such deviations? Noting that similar minima of regular ionic series are predicted by selectivity theory (Eisenman and Horn, 1983), a possible explanation of Fig. 6 is that these data reflect opposing influences of the size of the naked cations and the size and dehydration energies of hydrated cations. Given the ability of protonated amines to serve as hydrogen bond donors, it would be expected that MA, DMA, and TriMA are more "hydrated" in solution or interact more strongly with H_2O than TMA. This difference in hydrated size or dehydration energy could explain the ability of the largest molecule, TMA, to permeate more readily than the smaller molecules, DMA and TriMA. Other explanations based on specific chemical interactions with pore residues could also be proposed.

Whatever the explanation, it is evident that molecular size is not the sole factor that determines the relative permeability of substrate molecules in the DEAA mutant. After substitution of the Lys(III) residue by Ala, the mutated pore loses ionic selectivity and exhibits a larger molecular weight cutoff. This circumstance allows us to examine the permeability behavior of many more molecules than is possible for the native channel. The results show that the DEAA mutant still appears to exhibit certain chemical preferences for its organic substrates. These data do not allow us to define a discrete molecular size cutoff for this channel since the largest tested cation (TEA, minimum diameter = 8.2 Å) has a substantial permeability. In perusing the data of Fig. 10, one may be tempted to consider whether the DEAA channel has simply become a "big hole" with a diameter in excess of 10 Å, or has somehow acquired an "elasticity" that enables many large molecules to readily squeeze through the pore. This does not seem to be the case since the guanidinium toxins, TTX and STX, do block the channel, albeit with low affinity (Fig. 9 *A*). These cationic toxins have an effective diameter of 10–11 Å in their narrowest orientation and would be expected to pass through such a big hole or an elastic channel. Furthermore, the smaller cations, Tris and methylguanidine, are clearly less permeant than TEA. This shows that significant barriers to small molecule influx must still be present. Thus, we conclude that the DEAA Na^+ channel mutant is a "large pore," rather similar to the native Ca^{2+} channel (McCleskey and Almers, 1985), but retains an ability to discriminate among certain large cations by chemical interactions.

The bar graph of Fig. 10 *B* is meant to illustrate the organic cation results from the standpoint of the DEKA mutations. Here we see that mutation of Lys(III) to Ala greatly increases the permeability to three tested cations that are permeable through the native channel (NH_4^+, NH_3OH^+, guanidine) and also renders the channel newly permeable to 10 tested cations that do not pass through the wild type (MA, EA, DMA, EAOH, aminoguanidine, TriMA, TMA, Tris, choline, TEA). This figure also shows that simultaneous mutation of the three charged residues of the DEKA locus to Ala in

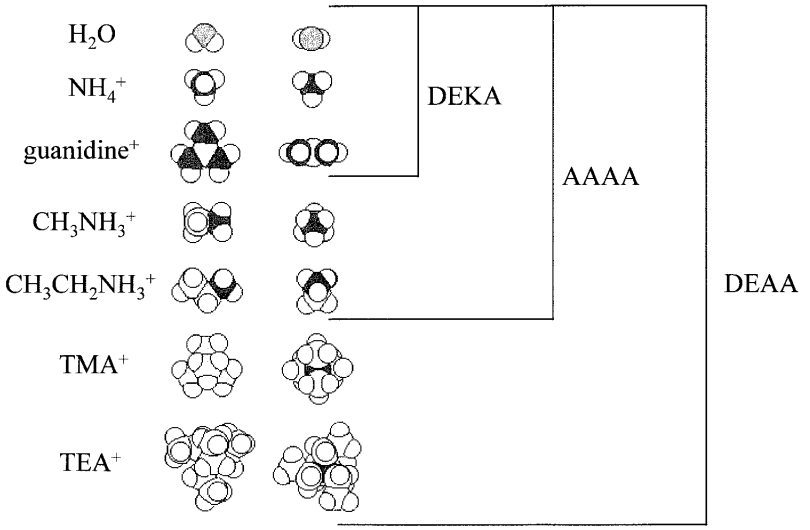

FIGURE 11. Space-filling models of several molecules illustrating the relative increase in cutoff diameter for AAAA and DEAA mutant Na^+ channels. Molecular models of the indicated molecules were constructed and energy minimized with the use of Hyperchem software. The seven molecules are arranged in order of increasing size from H_2O (*top*) to TEA (*bottom*). Two different views of each molecule are shown to indicate possible size constraints for permeation. Brackets on the right enclose the group of molecules that are permeable through each type of channel.

the AAAA mutant increases permeability to NH_4^+, NH_3OH^+, and guanidine, but only creates new permeability to MA and EA. Fig. 11 illustrates these observed changes in molecular cutoff behavior by comparing space-filling models of water and six tested cations that are respectively permeant in the wild-type channel and the AAAA and DEAA mutants. If the amino acid side chains of the DEKA locus behaved simply as an inert lining of the pore sieving region, one would have expected the AAAA mutant to have greater permeability for all of the same molecules that can permeate through DEAA. As calculated from the van der Waals volume of amino acid side chains, mutation of Lys to Ala removes ~56 Å^3 of molecular volume, whereas the combined mutation of Asp, Glu, and Lys to Ala removes ~110 Å^3. Thus, with respect to molecular sieving of organic cations, the side chains of the DEKA residues do not simply appear to operate as bulk mass that occludes the channel and clogs the pore. Rather, the results again point to the conclusion that molecular sieving by the DEKA residues is also governed by chemical and electrostatic interactions.

Consideration of the findings for the DAAA and AEAA mutants (Table II) further suggests that synergistic interactions among the DEKA residues may be important. For example, DAAA and AEAA have essentially the same permeability ratio for the methylated ammonium cations as AAAA. This implies that the simultaneous presence of the two negatively charged side chains at Asp(I) and Glu(II) is a necessary factor that makes the DEAA mutant newly permeable to many more organic cations. One possible explanation of these data is that the effective pore aperture may depend on electrostatic interactions at the DEKA locus. Electrostatic repulsion between negatively charged Asp(I) and Glu(II) side chains in the DEAA mutant may lead to structural changes that widen the aperture. The presence of the positively charged Lys(III) residue may partially cancel this repulsive interaction, causing the aperture to constrict. The relatively smaller cutoff diameter of the AAAA mutant may be explained by charge neutralization of the DEKA locus and the decreased polarity resulting from substitution of the methyl side chain of Ala for the three charged residues. As a precedent for this possibility, mutational analysis of the Tris/Na^+ permeability ratio in the acetylcholine receptor has shown that there is a negative correlation between the hydrophobicity of pore lining residues and the permeability of a large organic cation such as $Tris^+$ (Cohen et al., 1992). In this latter study, the authors also concluded that organic cation permeability is not simply related to the side chain volume of pore lining residues.

Block by Ca^{2+}, H^+, and the Gating-shift Phenomenon

A distinctive feature of Ca^{2+} channel permeation is block of currents of Na^+ and Li^+ by low concentrations of external divalent cations such as Ca^{2+} and Cd^{2+}. Mutational studies of the EEEE residues of Ca^{2+} channels imply that these four glutamate residues serve as the principal carboxylate ligands that mediate high affinity binding of Ca^{2+}/Cd^{2+} for this effect (Yang et al., 1993; Kim et al., 1993; Ellinor et al., 1995; Parent and Gopalakrishnan, 1995). This raises the question of what role do the DEKA residues have in mediating the low affinity blocking effect of extracellular Ca^{2+} on Na^+ channels?

This is not an easy question to address at the level of macroscopic current since the effects of external Ca^{2+} are complex. External Ca^{2+} in the millimolar range is known to cause a voltage-dependent "fast block" manifested as a decrease in unitary conductance. External Ca^{2+} is also known to strongly shift the voltage dependence of activation to more positive voltages. Arm-

strong and Cota (1991) have proposed that these two different effects may be mediated by binding of Ca^{2+} at a common site in the pore. Here we investigated whether the DEKA residues are involved in these phenomena by analyzing the macroscopic peak I–V relations. The present method does not allow us to accurately extract the voltage dependence of Ca^{2+} block but it provides some information on relative Ca^{2+} blocking affinity in the positive voltage range. For example, in Zn^{2+}-sensitive isoforms and mutants of the Na^+ channel, inhibition of the G_{max} parameter by external Zn^{2+} is very well correlated with the blocking effect of Zn^{2+} measured at the single-channel level (Schild et al., 1991; Favre et al., 1995). This provides us with a good rationale for considering the reduction in G_{max} as a relative measure of block in the positive voltage range.

Fig. 3 *C* compares the titration of 1 to 31 mM Ca^{2+} on G_{max} for the Ca^{2+}-impermeant DEKA wild-type and AAAA channels. On the likely assumption that the ~45% decrease in G_{max} of the wild-type channel is primarily a reflection of Ca^{2+} block, it appears that this blocking effect is practically eliminated in the AAAA mutant. A possible interpretation of this result is that low affinity Ca^{2+} block of Na^+ current in the native channel occurs by weak binding of Ca^{2+} in the direct vicinity of the DEKA locus, perhaps by weak coordination to oxygen atoms of the Asp(I) and Glu(II) residues. Since these acidic residues are missing in the AAAA channel, this Ca^{2+}-binding site would be eliminated in this mutant. The very weak Ca^{2+}-blocking activity remaining in the Ca^{2+}-impermeant AAAA mutant could be mediated by Ca^{2+} binding to other sites, and perhaps also by screening of negative surface potential generated by other acidic residues in the outer vestibule; e.g., at the outer ring of negative charge identified by Terlau et al. (1991). The situation for the DEAA mutant is more difficult to interpret because this channel is highly permeable to Ca^{2+} as demonstrated by the Ca^{2+}-dependent shift of the reversal potential (Fig. 3 *D*). To analyze Ca^{2+}-blocking behavior in this and other Ca^{2+}-permeable mutants, it will be necessary to investigate the effects of submillimolar divalent cation concentrations. This may reveal whether mutation of the Lys(III) residue to Ala leads to the acquisition of high affinity divalent cation block as previously observed for DEEA, DEEE, and similar mutants of the rat brain Na^+ channel (Heinemann et al., 1992; Schlief et al., 1996).

Another interesting observation is that the AAAA mutant exhibits practically the same Ca^{2+} dependence for the midpoint of voltage activation as that of the native channel, aside from an absolute displacement of ~+10 mV (Fig. 3 *E*). Following from the above interpretation of the G_{max} data, this implies that the low affinity Ca^{2+}-blocking site does not directly mediate the gating shift phenomenon and argues against the proposal that Ca^{2+} block and gating-shift are simply manifestations of the same site of action (Armstrong and Cota, 1991). One plausible interpretation of the $V_{0.5}$ data in Fig. 3 *E* is that the charges of the DEKA residues themselves have a small intrinsic influence (~+10 mV) on the midpoint of voltage activation, but that the gating-shift effect of external Ca^{2+} is mediated by Ca^{2+}-dependent neutralization (via binding and screening) of other negative surface charges located elsewhere on the channel protein and/or phospholipids (Cukierman et al., 1988). The data of Fig. 3 *D* also indicates that the Ca^{2+} shift of $V_{0.5}$ for the DEAA mutant saturates at a significantly more negative voltage than that for the wild-type and AAAA mutants. While we do not understand the basis for this effect, it might be due to changes in channel gating resulting from Ca^{2+} accessibility to internal sites in the pore.

A related question explored in this paper is the role of the DEKA residues in mediating block by external H^+ and/or the H^+-dependent gating shift. The results of Fig. 4 *C* show the H^+-dependent shift of the macroscopic $V_{0.5}$ parameter for voltage activation is very similar in the DEAA and AAAA mutants as compared with the wild-type channel. This rules out a major involvement of these residues in this particular effect. However, there does appear to be an effect on external block by H^+ as monitored at the macroscopic level by pH-dependent inhibition of G_{max}. Fig. 4 *D* shows that the AAAA mutant is significantly less sensitive to inhibition by low external pH than the wild-type and DEAA channels. The data for the AAAA mutant implies that there is a small shift of the apparent pKa of channel inhibition to lower pH values and that a fraction (~37%) of the total conductance is resistant to H^+ block at pH 4.0.

Our interpretation of these results is that macroscopic H^+ block is due to protonation of multiple residues in the outer vestibule (Mozhayeva et al., 1981). In this model, Ala substitution of the Asp(I), Glu(II), and Lys(III) residues of the DEKA locus would eliminate or dissect out the effect of H^+ protonation at these particular residues and reveal the separate contribution of other negatively charged carboxyl groups, perhaps those at the outer ring of charge (Terlau et al., 1991). In essence, we infer that H^+ block in this mutant causes an H^+-resistant subconductance state similar to the effects described for various mutations of the Ca^{2+} channel where Glu residues of the EEEE locus are neutralized by substitution with Glu (Chen et al., 1996). The observed decrease in the macroscopic pKa by ~0.3 pH units for AAAA relative to the DEAA mutant is consistent with a reduction in negative surface potential that lowers the pKa of the remaining H^+-titratable sites in the outer vestibule by an electrostatic effect (Sternberg et al., 1987). However, electrostatic considerations do not provide an obvious explanation for the small de-

crease in the apparent pKa of the DEAA mutant relative to the wild-type DEKA channel. Simple neutralization of a positively charged Lys residue in the external vestibule would be expected to make the surface potential slightly more negative, which should increase the apparent pKa according to the conventional theory of H^+ titration of surface groups. Nevertheless, the results of Fig. 4 do identify a contribution of the charged residues of the DEKA locus to the phenomenon of external H^+ block of the μ1 Na^+ channel.

Is the DEKA Locus the Selectivity Filter?

As introduced above, the concept of a selectivity filter is based on the theoretical notion that highly ion-selective channels must have a narrow region where chemical groups of the channel wall can directly interact with substrate ions to energetically favor or disfavor their passage (Eisenman and Dani, 1987; Hille, 1992). This assumption leads to the prediction that if a particular part of the channel functions in the role of a selectivity filter, then this structure must also function in molecular sieving. However, hunting for the selectivity filter by mutational analysis is not as straightforward as it sounds. Once the suspected residues are found, the question becomes, "how do we know that this is it?" Any alteration in protein structure that indirectly perturbs the pore could be mistaken for a direct effect on the filter.

The DEKA locus of the Na^+ channel was originally identified by mutational scanning of the four homologous P-region segments in subdomains I–IV (Terlau et al., 1991; Heinemann et al., 1992). The hypothesis originating from this work, that these particular residues comprise the structural equivalent of a selectivity filter; i.e., that they are oriented within close proximity in a ringlike configuration and that they are principal determinants of ionic selectivity and ion blocking affinity, is now supported by a variety of complementary mechanistic studies on the homologous DEKA/EEEE loci of Na^+ channels/Ca^{2+} channels (Heinemann et al., 1992, 1994; Yang et al., 1993; Ellinor et al., 1995; Favre et al., 1996; Schlief et al., 1996). Cysteine-scanning mutagenesis has also implicated the involvement of other P-region residues such as Trp1531, Asp1532, and Gly1533 in subdomain IV of the μ1 Na^+ channel as possible determinants of ionic selectivity (Tsushima et al., 1997; Chiamvimonvat et al., 1996). However, analogous Cys mutations of these latter subdomain IV residues in the human heart Na^+ channel do not have significant effects on group IA cation selectivity (Chen et al., 1977), suggesting that these particular residues may not play a universal or fundamental role in Na^+ channel selectivity.

To summarize the present study, macroscopic electrophysiological analysis of Ala mutations of the charged residues of the DEKA locus of μ1 Na^+ channels expressed in HEK293 cells confirmed the functional significance of these residues as previously deduced by heterologous expression in *Xenopus* oocytes (Favre et al., 1996; Heinemann et al., 1992). The results shown here further establish a pivotal role of the Lys(III) residue in the mechanism of ionic selectivity among the series of five group IA monovalent cations and in preventing the permeation of four group IIA divalent cations. In addition, the prediction that the DEKA residues would be important for molecular sieving of organic cations was verified. The results suggest that these residues cooperate to determine the molecular cutoff diameter for diffusion of organic cations through the Na^+ channel pore. Organic cation permeation in Ala mutants of the DEKA locus appears to depend in a complex manner on specific chemical and electrostatic interactions with substrate molecules. The results also suggest that the DEKA locus is involved in the mechanism of external Ca^{2+} block and external H^+ block. If these permeability functions are taken as the hallmark of a putative selectivity filter, then the DEKA locus must be considered as a serious candidate for that structure.

The authors thank Maria Morabito for help with some of the subcloning procedures.

This research was supported by grants from the National Institutes of Health (GM-51172 to E. Moczydlowski) and from the Swiss National Science Foundation (31-39435 to L. Schild).

Original version received 8 July 1997 and accepted version received 15 September 1997.

REFERENCES

Almers, W., and E.W. McCleskey. 1984. Non-selective conductance in calcium channels of frog muscle: calcium selectivity in a single-file pore. *J. Physiol. (Lond.).* 353:585–608.

Almers, W., E.W. McCleskey, and P.T. Palade. 1984. A non-selective cation conductance in frog muscle membrane blocked by micromolar external calcium ions. *J. Physiol. (Lond.).* 353:565–583.

Armstrong, C.M., and G. Cota. 1991. Calcium ion as a cofactor in Na channel gating. *Proc. Natl. Acad. Sci. USA.* 88:6528–6531.

Armstrong, C.M., and W.F. Gilly. 1992. Access resistance and space clamp problems associated with whole-cell patch clamping. *Methods Enzymol.* 207:100–122.

Becker, S., E. Prusak-Sochaczewski, G. Zamponi, A.G. Beck-Sick-

inger, R.D. Gordon, and R.J. French. 1992. Action of derivatives of μ-conotoxin GIIIA on sodium channels. Single amino acid substitutions in the toxin separately affect association and dissociation rates. *Biochemistry.* 31:8229–8238.

Behrens, M.I., A. Oberhauser, F. Bezanilla, and R. Latorre. 1989. Batrachotoxin-modified sodium channels from squid optic nerve in planar bilayers: ion conduction and gating properties. *J. Gen. Physiol.* 93:23–41.

Bezanilla, F., and C.M. Armstrong. 1972. Negative conductance caused by entry of sodium and cesium ions into the potassium channels of squid axons. *J. Gen. Physiol.* 60:588–608.

Campbell, D.T. 1976. Ionic selectivity of the sodium channel of frog skeletal muscle. *J. Gen. Physiol.* 67:295–307.

Campbell, D.T., and B. Hille. 1976. Kinetic and pharmacological properties of the sodium channel of frog skeletal muscle. *J. Gen. Physiol.* 67:309–323.

Chanine, M., L.-Q. Chen, N. Fotouhi, R. Walsky, D. Fry, V. Santarelli, R. Horn, and R.G. Kallen. 1995. Characterizing the μ-conotoxin binding site on voltage-sensitive sodium channels with toxin analogs and channel mutations. *Receptors Channels.* 3:161–174.

Chen, C., and H. Okayama. 1987. High-efficiency transformation of mammalian cells by plasmid DNA. *Mol. Cell. Biol.* 7:2745–2752.

Chen, S.-F., H.A. Hartmann, and G.E. Kirsch. 1997. Cysteine mapping in the ion selectivity and toxin binding region of the cardiac Na^+ channel pore. *J. Membr. Biol.* 155:11–25.

Chen, X.-H., I. Bezprozvanny, and R.W. Tsien. 1996. Molecular basis of proton block of L-type Ca^{2+} channels. *J. Gen. Physiol.* 108: 363–374.

Chiamvimonvat, N., M.T. Perez-Garcia, R. Ranjan, E. Marban, and G.F. Tomaselli. 1996. Depth asymmetries of the pore-lining segments of the Na^+ channel revealed by cysteine mutagenesis. *Neuron.* 16:1037–1047.

Cohen, B.N., C. Labarca, L. Czyzyk, N. Davidson, and H.A. Lester. 1992. $Tris^+/Na^+$ permeability ratios of nicotinic acetylcholine receptors are reduced by mutations near the intracellular end of the M2 region. *J. Gen. Physiol.* 99:545–572.

Coronado, R., and J.S. Smith. 1987. Monovalent ion current through single calcium channels of skeletal muscle transverse tubules. *Biophys. J.* 51:497–502.

Cukierman, S., W.C. Zinkand, R.J. French, and B.K. Krueger. 1988. Effects of membrane surface charge and calcium on the gating of rat brain sodium channels in planar bilayers. *J. Gen. Physiol.* 92: 431–447.

Daumas, P., and O.S. Andersen. 1993. Proton block of rat brain sodium channels: evidence for two proton binding sites and multiple occupancy. *J. Gen. Physiol.* 101:27–43.

Dudley, S.C.J., H. Todt, G. Lipkind, and H.A. Fozzard. 1995. A μ-conotoxin-insensitive Na^+ channel mutant: possible localization of a binding site in the outer vestibule. *Biophys. J.* 69:1657–1665.

Dwyer, T.M., D.J. Adams, and B. Hille. 1980. The permeability of the endplate channel to organic cations in frog muscle. *J. Gen. Physiol.* 75:469–492.

Dwyer, T.M., and J.M. Farley. 1984. Permeability properties of chick myotube acetycholine-activated channels. *Biophys. J.* 45:529–539.

Eisenman, G., and R. Horn. 1983. Ionic selectivity revisited: the role of kinetic and equilibrium processes in ion permeation through channels. *J. Membr. Biol.* 76:197–225.

Eisenman, G., and J.A. Dani. 1987. An introduction to molecular architecture and permeability of ion channels. *Annu. Rev. Biophys. Biophys. Chem.* 16:205–226.

Ellinor, P.T., J. Yang, W.A. Sather, J.-F. Zhang, and R.W. Tsien. 1995. Ca^{2+} channel selectivity at a single locus for high-affinity Ca^{2+} interactions. *Neuron.* 15:1121–1132.

Favre, I., E. Moczydlowski, and L. Schild. 1995. Specificity for block by saxitoxin and divalent cations at a residue which determines sensitivity of sodium channel subtypes to guanidinium toxins. *J. Gen. Physiol.* 106:203–229.

Favre, I., E. Moczydlowski, and L. Schild. 1996. On the structural basis for ionic selectivity among Na^+, K^+, and Ca^{2+} in the voltage-gated sodium channel. *Biophys. J.* 71:3110–3125.

Frankenhaeuser, B., and A.L. Hodgkin. 1957. The action of calcium on the electrical properties of squid axons. *J. Physiol. (Lond.).* 137:218–244.

Goulding, E.H., G.R. Tibbs, D. Liu, and S.A. Siegelbaum. 1993. Role of H5 domain in determining pore diameter and ion permeation through cyclic nucleotide-gated channels. *Nature.* 364: 61–64.

Heinemann, S.H., H. Terlau, W. Stühmer, K. Imoto, and S. Numa. 1992. Calcium channel characteristics conferred on the sodium channel by single mutations. *Nature.* 356:441–443.

Heinemann, S.H., T. Schlief, Y. Mori, and K. Imoto. 1994. Molecular pore structure of voltage-gated sodium and potassium channels. *Braz. J. Med. Biol. Res.* 27:2781–2802.

Hess, P., and R.W. Tsien. 1984. Mechanism of ion permeation through calcium channels. *Nature (Lond.).* 309:453–456.

Hille, B. 1971. The permeability of the sodium channel to organic cations in myelinated nerve. *J. Gen. Physiol.* 58:599–619.

Hille, B. 1972. The permeability of the sodium channel to metal cations in myelinated nerve. *J. Gen. Physiol.* 59:637–658.

Hille, B. 1973. Potassium channels in myelinated nerve. Selective permeability to small cations. *J. Gen. Physiol.* 61:669–686.

Hille, B. 1992. Ionic Channels of Excitable Membranes. 2nd ed. Sinauer Associates, Inc., Sunderland, MA. 607 pp.

Hille, B., A.M. Woodhull, and B.I. Shapiro. 1975. Negative surface charge near sodium channels of nerve: divalent ions, monovalent ions, and pH. *Philos. Trans. R Soc. Lond. B Biol. Sci.* 270:301–318.

Kim, M.-S., T. Mori, L.-X. Sun, K. Imoto, and Y. Mori. 1993. Structural determinants of ion selectivity in brain calcium channel. *FEBS Lett.* 318:145–148.

Kuo, C.-C., and P. Hess. 1993. Ion permeation through the L-type Ca^{2+} channel in rat phaeochromocytoma cells: two sets of ion binding sites in the pore. *J. Physiol. (Camb.).* 466:629–655.

Lancelin, J.-M., D. Kohda, S. Tate, Y. Yanagawa, T. Abe, M. Satake, and F. Inagaki. 1991. Tertiary structure of conotoxin GIIIA in aqueous solution. *Biochemistry.* 30:6908–6916.

Lewis, C.A. 1979. Ion-concentration dependence of the reversal potential and the single channel conductance of ion channels at the frog neuromuscular junction. *J. Physiol. (Camb.).* 286:417–445.

McCleskey, E.W., and W. Almers. 1985. The Ca channel in skeletal muscle is a large pore. *Proc. Natl. Acad. Sci. USA.* 82:7149–7153.

Mozhayeva, G.N., A.P. Naumov, and Y.A. Negulyaev. 1981. Evidence for existence of two acid groups controlling the conductance of sodium channel. *Biochim. Biophys. Acta.* 643:251–255.

Nilius, B. 1988. Calcium block of guinea-pig heart sodium channels with and without modification by the piperazynylindole DPI 201-106. *J. Physiol. (Camb.).* 399:537–558.

Pappone, P.A. 1980. Voltage-clamp experiments in normal and denervated mammalian skeletal muscle fibers. *J. Physiol. (Camb.).* 306:377–410.

Parent, L., and M. Gopalakrishnan. 1995. Glutamate substitution in repeat IV alters divalent and monovalent cation permeation in the heart Ca^{2+} channel. *Biophys. J.* 69:1801–1813.

Ravindran, A., L. Schild, and E. Moczydlowski. 1991. Divalent cation selectivity for external block of voltage-dependent Na^+ channels prolonged by batrachotoxin: Zn^{2+} induces discrete substates in cardiac Na^+ channels. *J. Gen. Physiol.* 97:89–115.

Sather, W.A., J. Yang, and R.W. Tsien. 1994. Structural basis of ion

channel permeation and selectivity. *Curr. Opin. Neurobiol.* 4:313–323.

Sato, K., Y. Ishida, K. Wakamatsu, R. Kato, H. Honda, Y. Ohizumi, H. Nakamura, M. Ohya, J.-M. Lancelin, D. Kohda, and F. Inagaki. 1991. Active site of μ-conotoxin GIIIA, a peptide blocker of muscle sodium channels. *J. Biol. Chem.* 266:16989–16991.

Schild, L., A. Ravindran, and E. Moczydlowski. 1991. Zn^{2+}-induced subconductance events in cardiac Na^+ channels prolonged by batrachotoxin: current-voltage behavior and single-chanel kinetics. *J. Gen. Physiol.* 97:117–142.

Schlief, T., R. Schönherr, K. Imoto, and S.H. Heinemann. 1996. Pore properties of rat brain II sodium channels mutated in the selectivity filter domain. *Eur. Biophys. J.* 25:75–91.

Sternberg, M.J.E., F.R.F. Hayes, A.J. Russell, P.G. Thomas, and A.R. Fersht. 1987. Prediction of electrostatic effects of engineering of protein charges. *Nature.* 330:86–88.

Tang, S., G. Mikala, A. Bahinski, A. Yatani, G. Varadi, and A. Schwartz. 1993. Molecular localization of ion selectivity sites within the pore of a human L-type cardiac calcium channel. *J. Biol. Chem.* 268:13026–13029.

Terlau, H., S.H. Heinemann, W. Stühmer, M. Pusch, F. Conti, K. Imoto, and S. Numa. 1991. Mapping the site of block by tetrodotoxin and saxitoxin of sodium channel II. *FEBS Lett.* 293:93–96.

Trimmer, J.S., S.S. Cooperman, S.A. Tomiko, J. Zhou, S.M. Crean, M.B. Boyle, R.G. Kallen, Z. Sheng, R.L. Barchi, F.J. Sigworth, R.H. Goodman, W.S. Agnew, and G. Mandel. 1989. Primary structure and functional expression of a mammalian skeletal muscle sodium channel. *Neuron.* 3:33–49.

Tsushima, R.G., R.A. Li, and P.H. Backx. 1997. Altered ionic selectivity of the sodium channel revealed by cysteine mutations within the pore. *J. Gen. Physiol.* 109:463–475.

Wang, F., and K. Imoto. 1992. Pore size and negative charge as structural determinants of permeability in the *Torpedo* nicotinic acetylcholine receptor channel. *Proc. R. Soc. Lond. B Biol. Sci.* 250: 11–17.

Woodhull, A.M. 1973. Ionic blockage of sodium channel in nerve. *J. Gen. Physiol.* 61:687–708.

Yamamoto, D., J.Z. Yeh, and T. Narahashi. 1984. Voltage-dependent calcium block of normal and tetramethrin-modified single sodium channels. *Biophys. J.* 45:337–344.

Yang, J., P.T. Ellinor, W.A. Sather, J.-F. Zhang, and R.W. Tsien. 1993. Molecular determinants of Ca^{2+} selectivity and ion permeation in L-type Ca^{2+} channels. *Nature.* 366:158–161.

Zhang, J.-F., and S.A. Siegelbaum. 1991. Effects of external protons on single cardiac sodium channels from guinea pig ventricular myocytes. *J. Gen. Physiol.* 98:1065–1083.